GM 73593

Technical report, geophysical data compilation, 3D magnetic data inversion, interpretation and targeting, Galactic project

Documents complémentaires

Additional Files

Licence

License

Ressources naturelles et Forêts
Québec

Technical Report

Geophysical data compilation, 3D magnetic data inversion, interpretation and targeting

Galactic Project
Sept-Îles Area, Côte-Nord Region, Québec
2024

NeoTerreX Minerals Inc.
Jens Hansen
François Desrosiers

Dynamic
Discovery
Geoscience

Prepared by
Joël Dubé, P.Eng.

February 2024

Dynamic Discovery Geoscience
7977 Décarie Drive
Ottawa (Ontario) K1C 3K3
jdube@ddgeoscience.ca

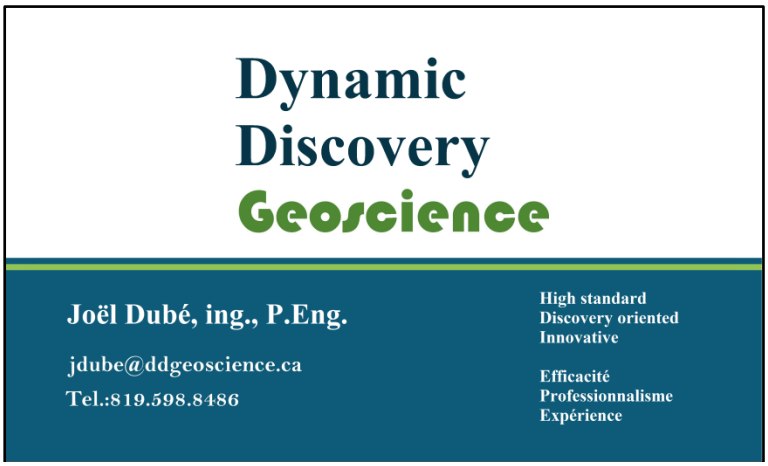

TABLE OF CONTENT

TABLES

FIGURES

I. INTRODUCTION

At the request of the mineral exploration company NeoTerreX Minerals Inc., and of the claims holders Jens Hansen and François Desrosiers, the firm Dynamic Discovery Geoscience Ltd. received the mandate to perform a geophysical data compilation, re-processing, interpretation and targeting, as well as 3D modeling of magnetic data available in the area of the Galactic Project (Figure 1).

The goal of this work was to search for geological and airborne geophysical data available in the area, to re-process and compile them in property scale maps and to perform interpretation of these data for the Galactic Project, with a focus on defining rare earth elements (REE) exploration targets. A secondary objective was to characterize the distribution of magnetic susceptibility within the 3D rock volume, in support of future follow-up work.

Figure 1: General location of the Galactic Project

II. GALACTIC PROJECT

The Galactic Project consists of a single block of mineral claims located about 45 km north of Part-Cartier and 55 km northwest of Sept-Îles, in the Côte-Nord Region, Province of Québec (Figure 2). The Property is found within NTS map sheet 022J06. Active mineral claim titles covered by the compilation, modeling and targeting work are shown in Figure 3 and listed in Table 1.

Figure 2: Regional location of the Galactic Project

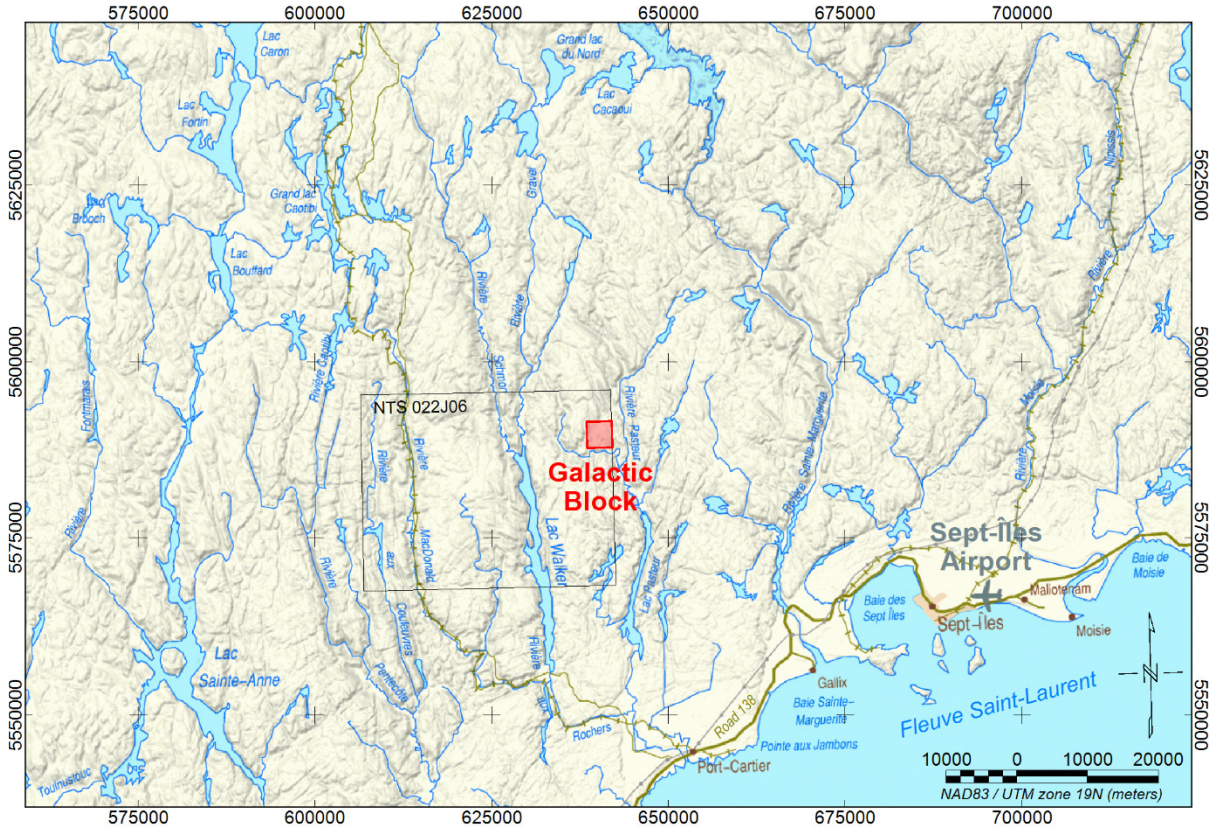

Table 1: Mineral claims covered by the work

Galactic Claim
2605859
2605860
2605861
2605862
2605863

Galactic Claim
2605864
2605865
2605866
2605867
2605868
2605882

Galactic Claim
2605883
2605884
2605885
2605886
2605887
2605888

Galactic Claim
2605889
2605890
2605891
2605892
2605893
2607162

III. DATA COMPILATION PRESENTATION

Geophysical data available

The airborne geophysical data used for the re-processing and compilation work are privately owned by NeoTerreX Minerals and were provided by its representative (Stephens, 2024). The magnetic and gamma-ray spectrometric data were acquired at a 10Hz sampling rate by Geo Data Solutions GDS Inc. in the month of October 2009. The survey was flown with a Robinson-R44 helicopter along lines oriented N090 and spaced every 100 m. Control lines were oriented perpendicular to traverse lines, at a 1000 m line spacing. The average height above ground of the helicopter and spectrometer was 46 m and the magnetic sensor was at 26 m. The average survey flying speed (calculated equivalent ground speed) was 34.5 m/s. The topography is locally very active with some challenging hills and depressions. The elevation is ranging from 144 to 519 m above mean sea level (MSL). Figure 3 indicates the survey flight lines, in black, on top of the Galactic claims, in red, and of the digital elevation model derived from the survey data.

The rest of this section presents the maps resulting from the geophysical data compilation and re-processing work performed.

Galactic_DEM map

This map shows the topography (digital elevation model from the 2009 survey in background) and puts the Project into geographical context. On this map, as well as on each of the other maps produced for this report, the following features are also shown:

- Mineral occurrences with rock sample assays in excess of 0.5% TREO (Total Rare Earth Elements, including Y) or of 0.4% Nb_2O_5, as reported in the work from Smith (2011) and Lavallée et al. (2011);
- Mineral claims under the control of NeoTerreX Minerals and its partners Jens Hansen and François Desrosiers;
- Geographical features made public by NRCan (roads, lakes, rivers, etc.).

Figure 3: Geographical data compilation

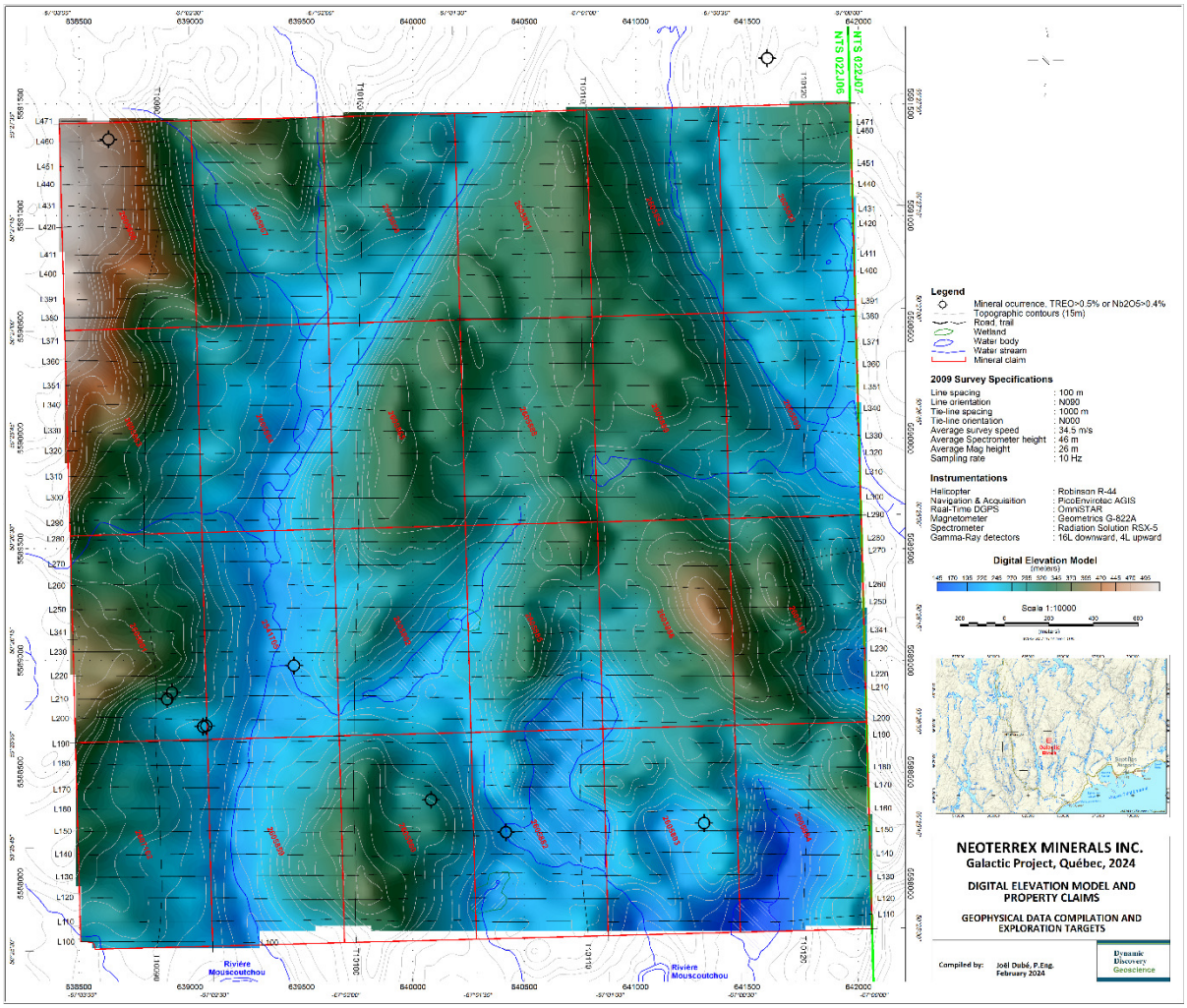

Galactic_TMI map

This map shows the residual Total Magnetic Intensity (TMI) from the airborne survey.

Figure 4: TMI data compilation, with equal area color distribution

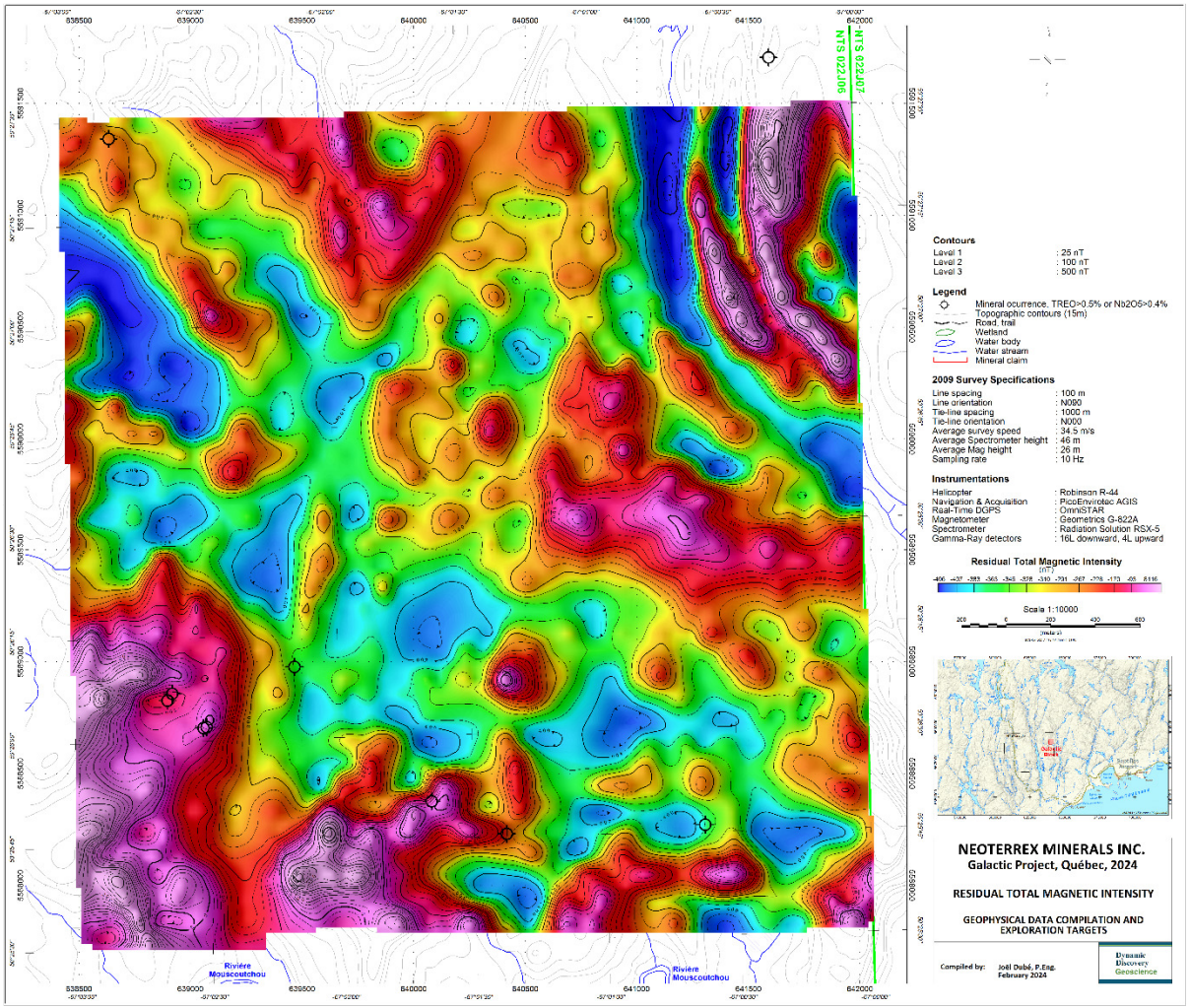

Galactic_FVD map

This map shows the First Vertical Derivative (FVD) of the TMI for the same magnetic survey. This product tends to highlight sources closer to surface and to narrow the outline of anomalies closer to the sources' extents. This is the preferred product for structural interpretation.

Figure 5: FVD data compilation

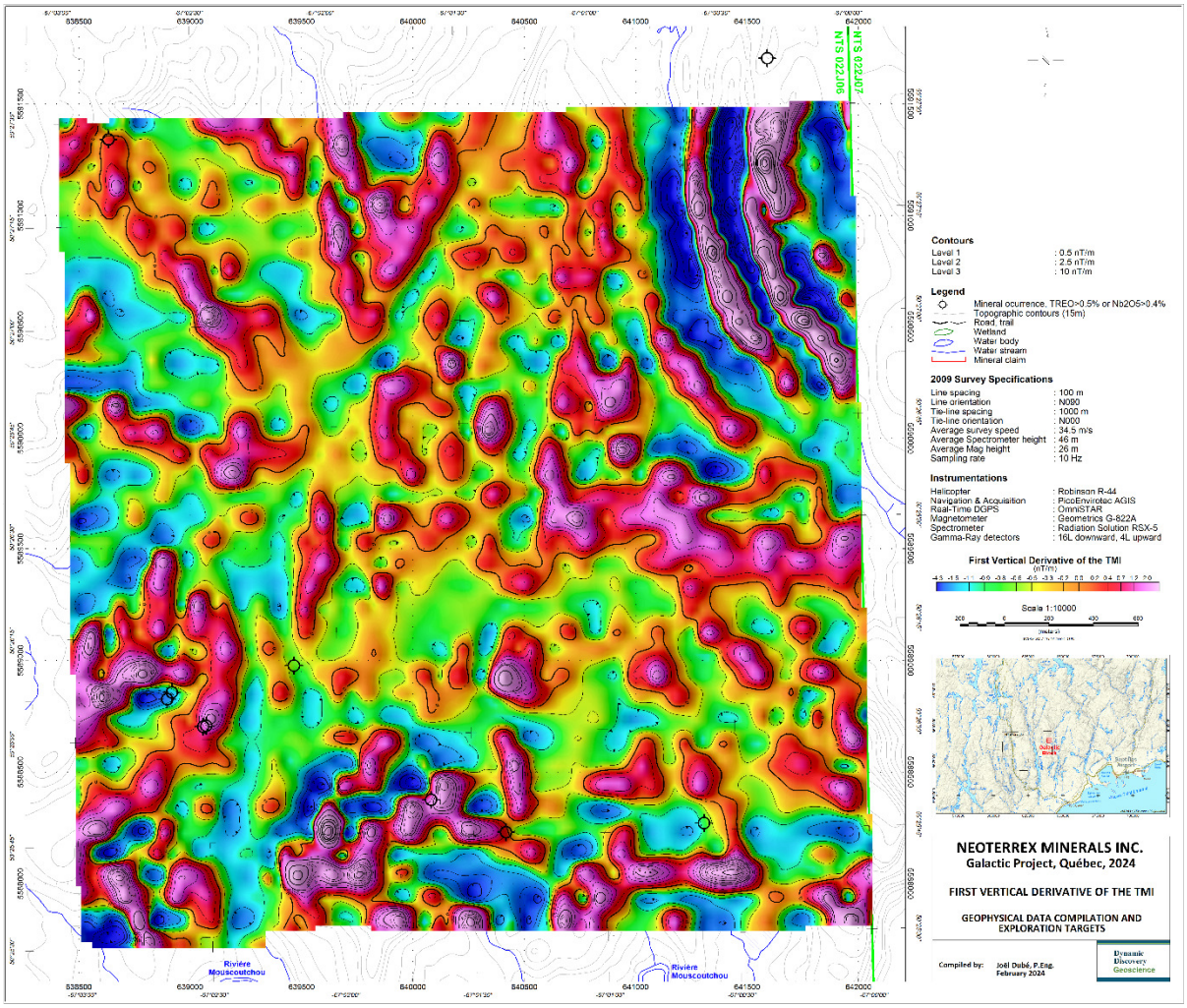

Galactic_TILT map

In order to enhance the subtle magnetic features some more, the Tilt Angle Derivative (TILT) was also computed for this project and is shown on this map. It has been shown that it is possible to use the Tilt Angle Derivative to estimate both the location and depth of magnetic sources as:

1- The 0° angle line is located directly above the contact between a magnetic source and the surrounding rock. This allows for accurate estimation of source location.

2- The distance between the 0° and the +45° contour lines as well as the distance between the -45° and the 0° contour lines are equal to the depth of the source at the contact. This allows for a direct estimation of the depth of the source of the anomaly. The depth estimated with this method is actually the distance between the magnetic sensor and the top of the source. Knowing that the sensor was 26 m above the ground in average enables direct depth estimates.

Figure 6: TILT data compilation

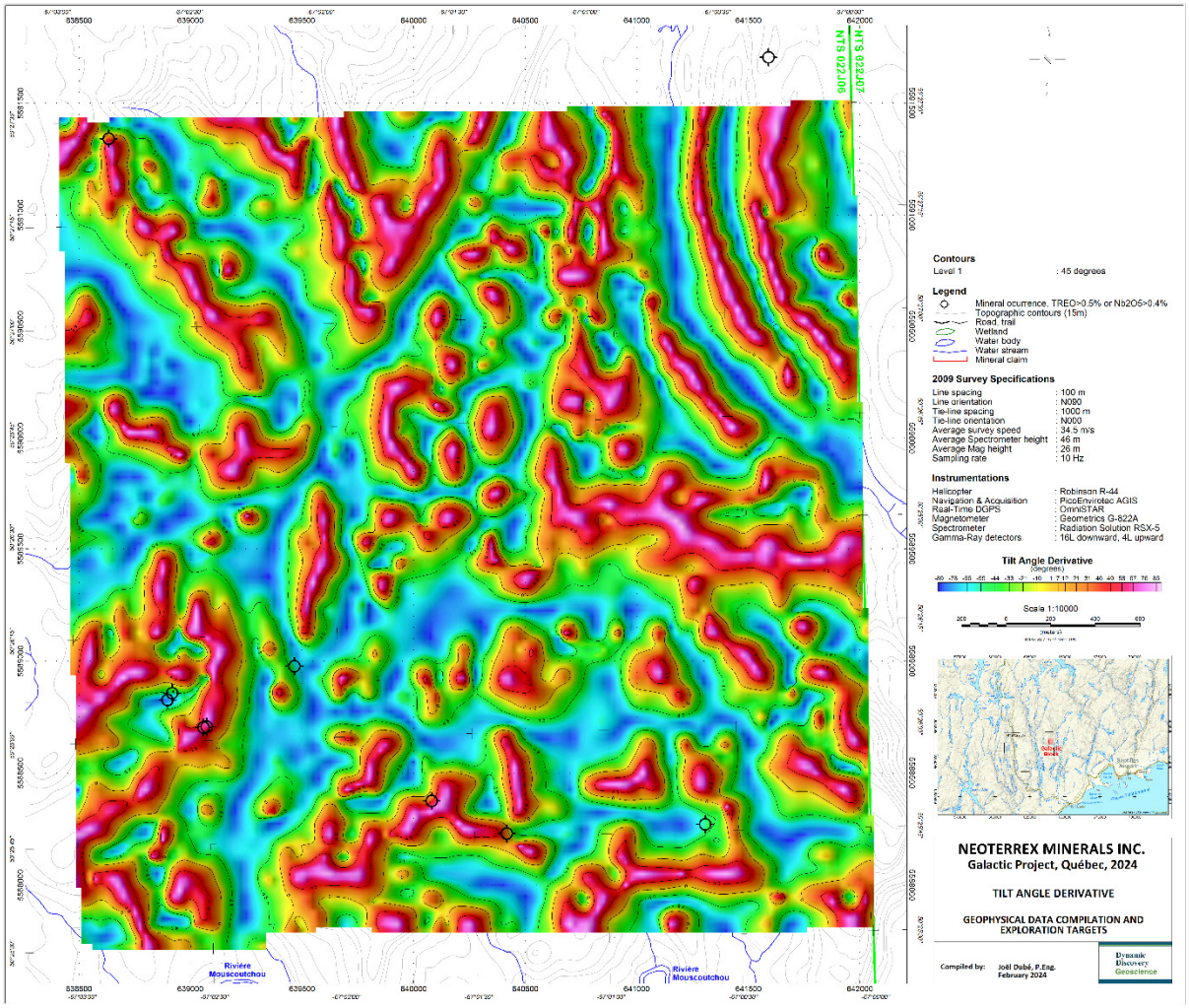

Galactic_TotalCount map

This map, sums up gamma-ray counts regardless of their radio-element nature. It is the radiometric product the least affected by noise and therefore highlights geological trends particularly well. Areas with strong total count anomalies have some potential to indicate hydrothermal events, since many radio-elements are often concentrated by these events or alteration phenomena related to them.

Figure 7: Gamma-ray Total Count data compilation

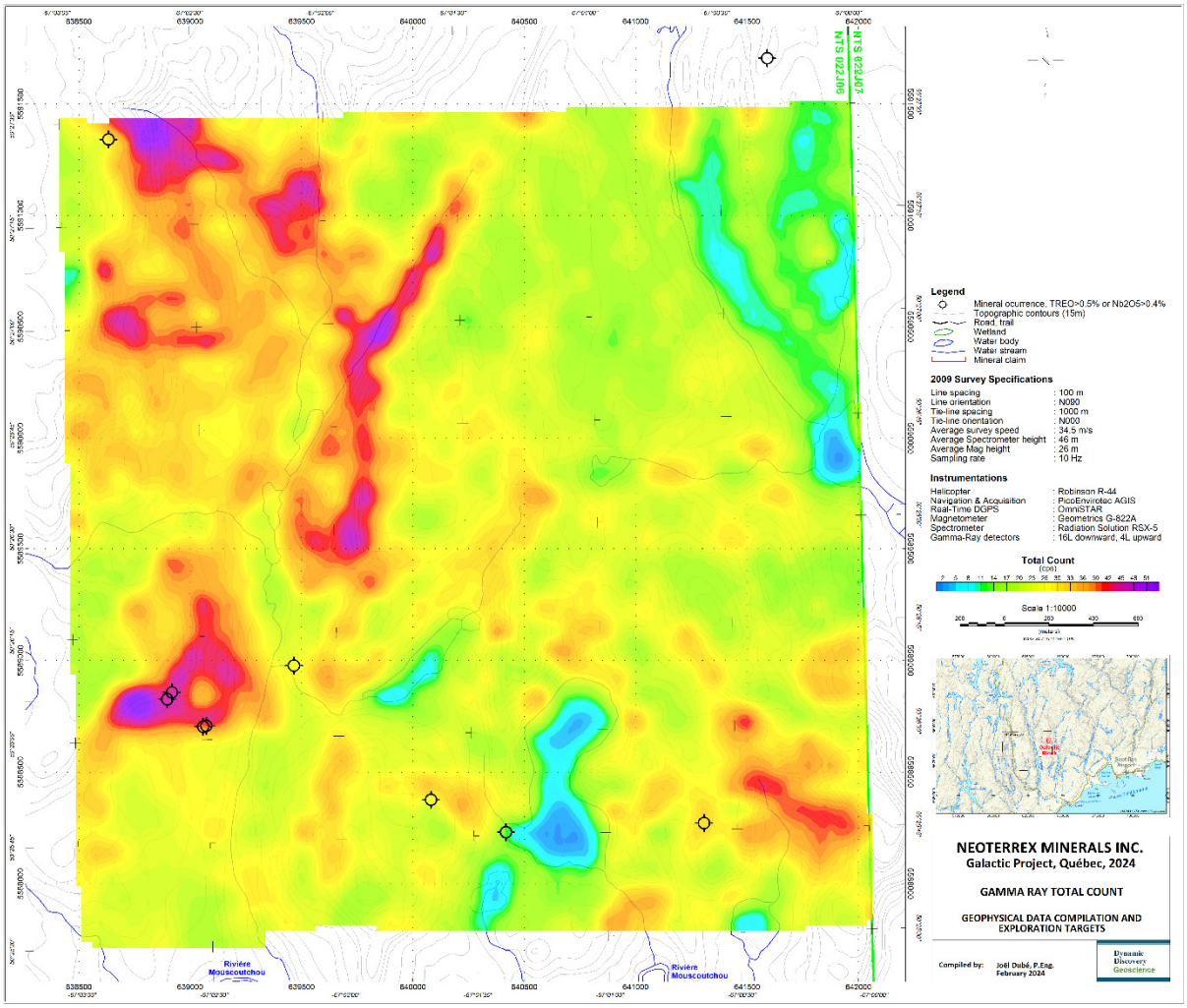

Galactic_Potassium

This map shows the Potassium concentration data compilation from the same survey. Since gamma-rays are quickly absorbed by matter, the response measured by the airborne system only comes from the first few centimeters of the ground. This has implications when interpreting spectrometric results and the radiometric method is therefore treated as a surficial exploration tool, with no penetration. Water accumulation in topographic lows attenuates most of the signal, and the response is thus partly controlled by non-geological elements. Nonetheless, it is a useful method for discriminating rock types on the basis of their radio-elements content, and can be used in support to geological mapping efforts. It is also an effective method at detecting specific rock alteration patterns. Since potassium alteration is known to be in relation with some gold deposits, such as in the case of the Hemlo deposit, or base metal occurrences, as is the case with porphyry copper or IOCG (Iron Oxide Copper-Gold, which can also include Fe-P-Cu-Au-Ag-U-F-REE) mineralization types, the potassium concentration data are considered as an important exploration tool in general.

Figure 8: Potassium data compilation

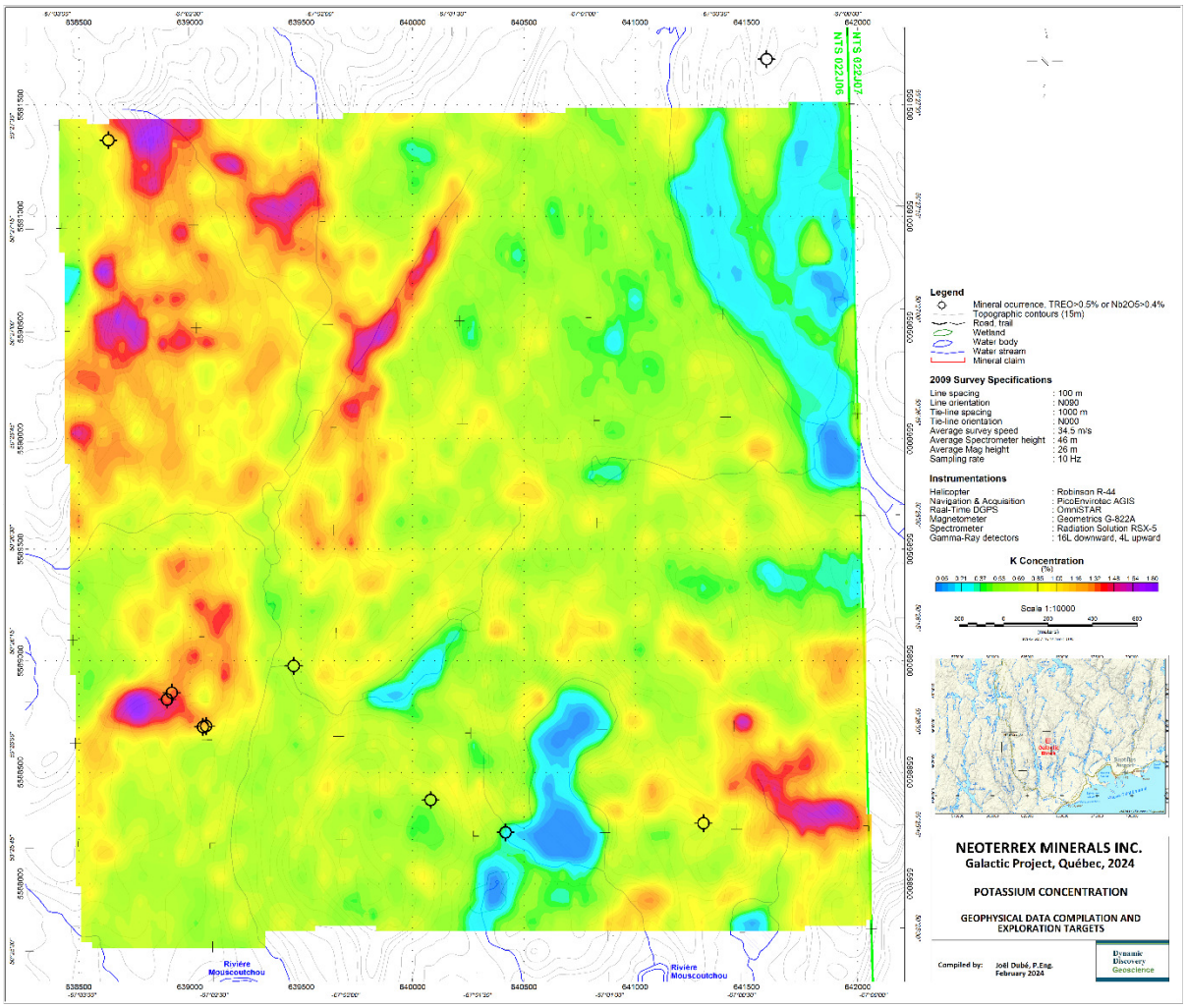

Galactic_eUranium

This map shows the equivalent Uranium (eUranium) concentration data compilation. These data are considered of interest in IOCG exploration contexts as well as for rare earth minerals exploration.

Figure 9: eUranium data compilation

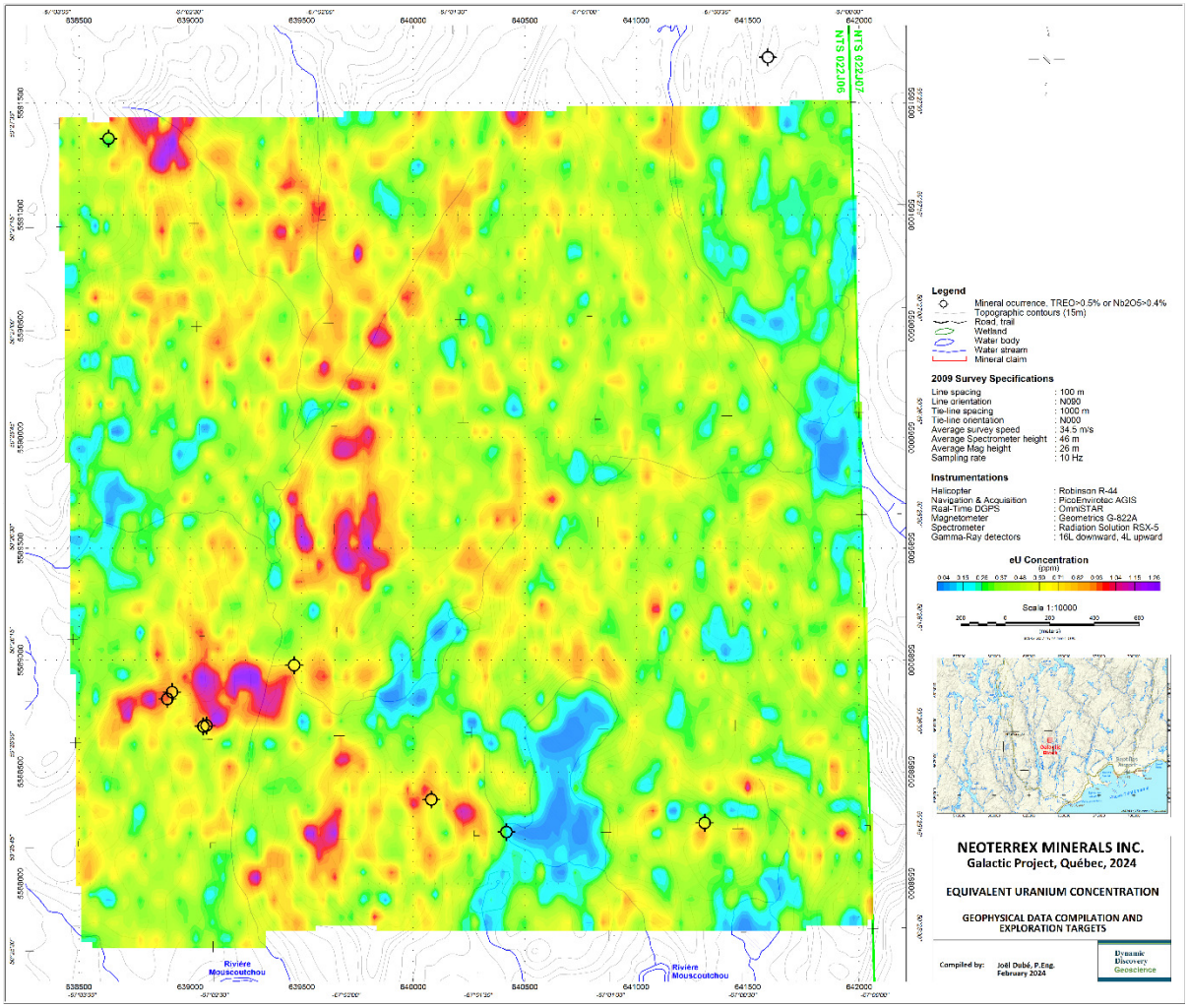

Galactic_eThorium

This map shows the equivalent Thorium (eThorium) concentration data compilation. These data are also considered of interest in IOCG exploration contexts and for rare earth minerals exploration.

Figure 10: eThorium data compilation

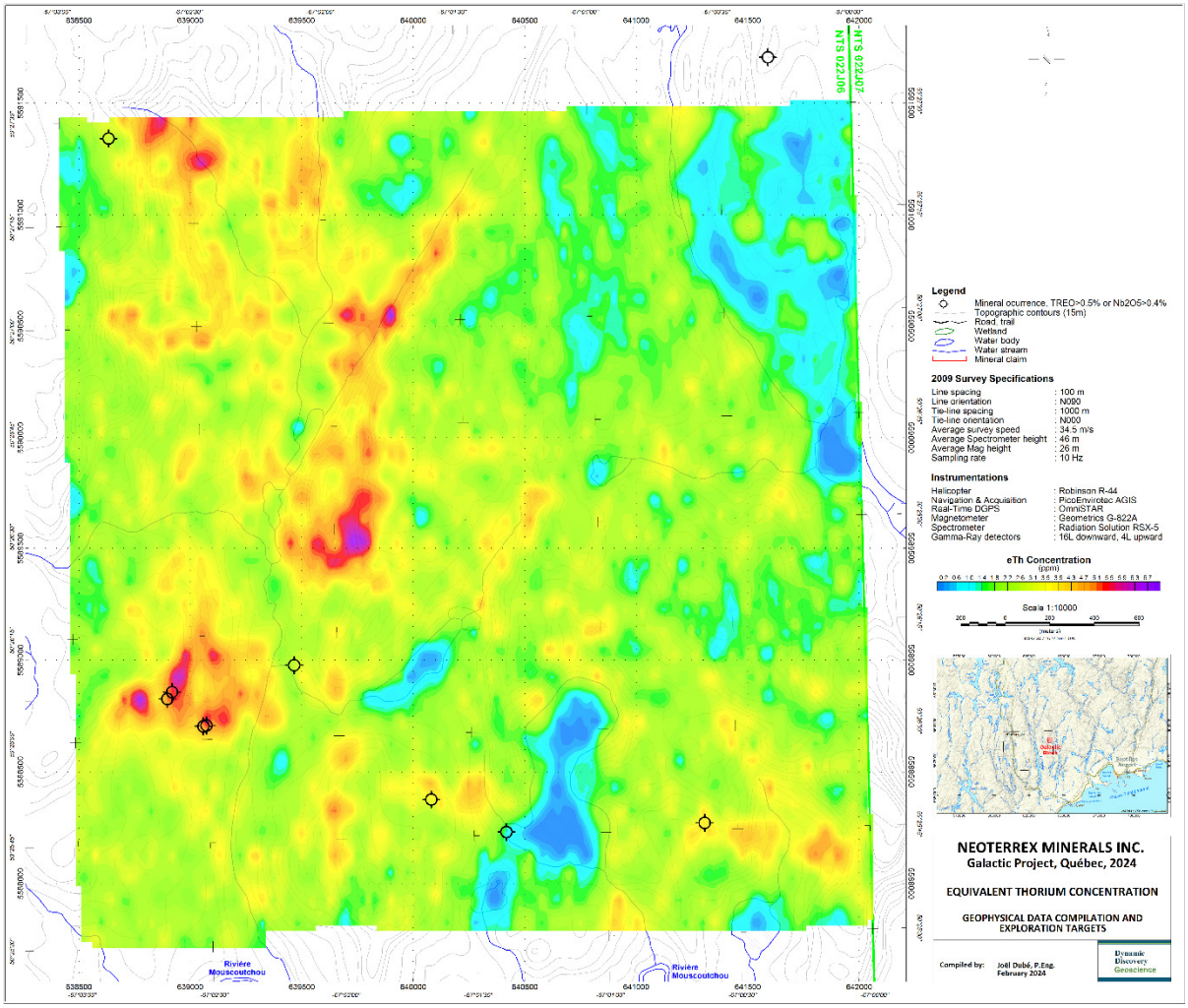

Galactic_ThKratio

This map shows the ratio of eThorium to Potassium. Interpretation based on ratios of radio-elements has advantages over the use of direct element concentration because natural variations from the level of rock exposition are adjusted for. Variable overburden thickness and extents, vegetation, topography and surface water content strongly control the intensity of gamma-rays response for all three elements. However, since radioactive elements are affected in the same manner by these variables, the ratios enable mitigation of these effects and enhance response from the geology. Ratio analysis is therefore preferred for elements with low natural concentrations such as Thorium. This said, ratios involving equivalent Uranium are however considered less reliable. This is because Uranium counts are generally very low, implying noisier data by nature, which usually results in very noisy calculated ratios. For this reason, ratios involving Uranium are not presented here in the report, but are delivered in the various grid formats nevertheless. Note that in the ratios data grids some areas do not have any data. This is done on purpose when the signal for one of the radio-elements is simply too low to yield a reliable ratio value.

Figure 11: Thorium/Potassium ratio data compilation

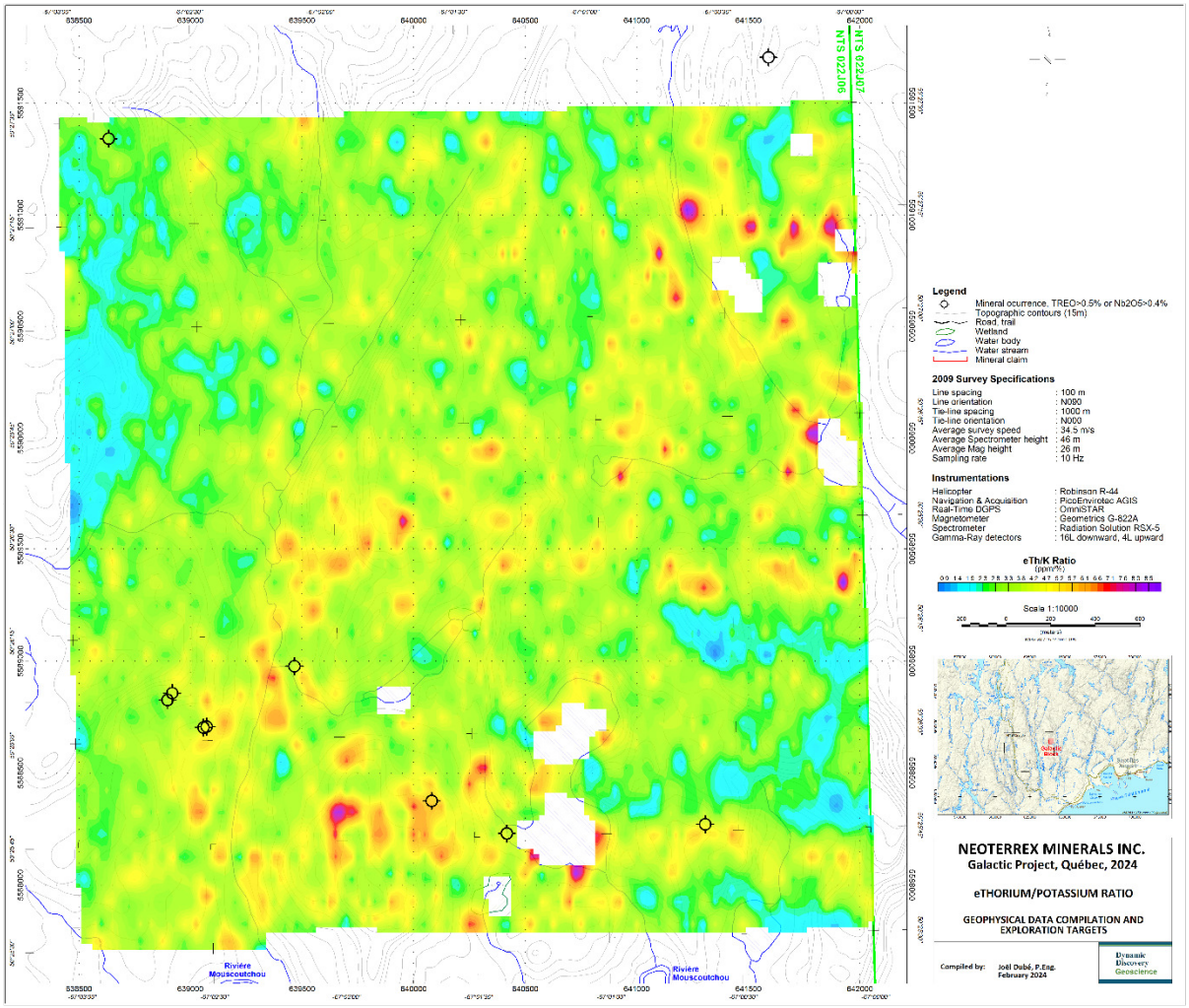

Galactic_TernarySpectro

The general response found in the block is variable for the three radio-elements analyzed. The spectrometric ternary image, which is shown on this map, is especially useful at identifying areas with radio-elements enrichment, and their associations/dissociations. The ternary image shows strong Potassium, Uranium and Thorium concentration in pink, light blue and yellow, respectively. Uranium-Thorium, Thorium-Potassium and Potassium-Uranium associations appear in green, red and dark blue, respectively. Areas with stronger concentrations in all elements are shaded darker and areas with weaker concentrations are shown in lighter colors, almost white in some places, such as over lakes.

Figure 12: Spectrometric ternary image data compilation

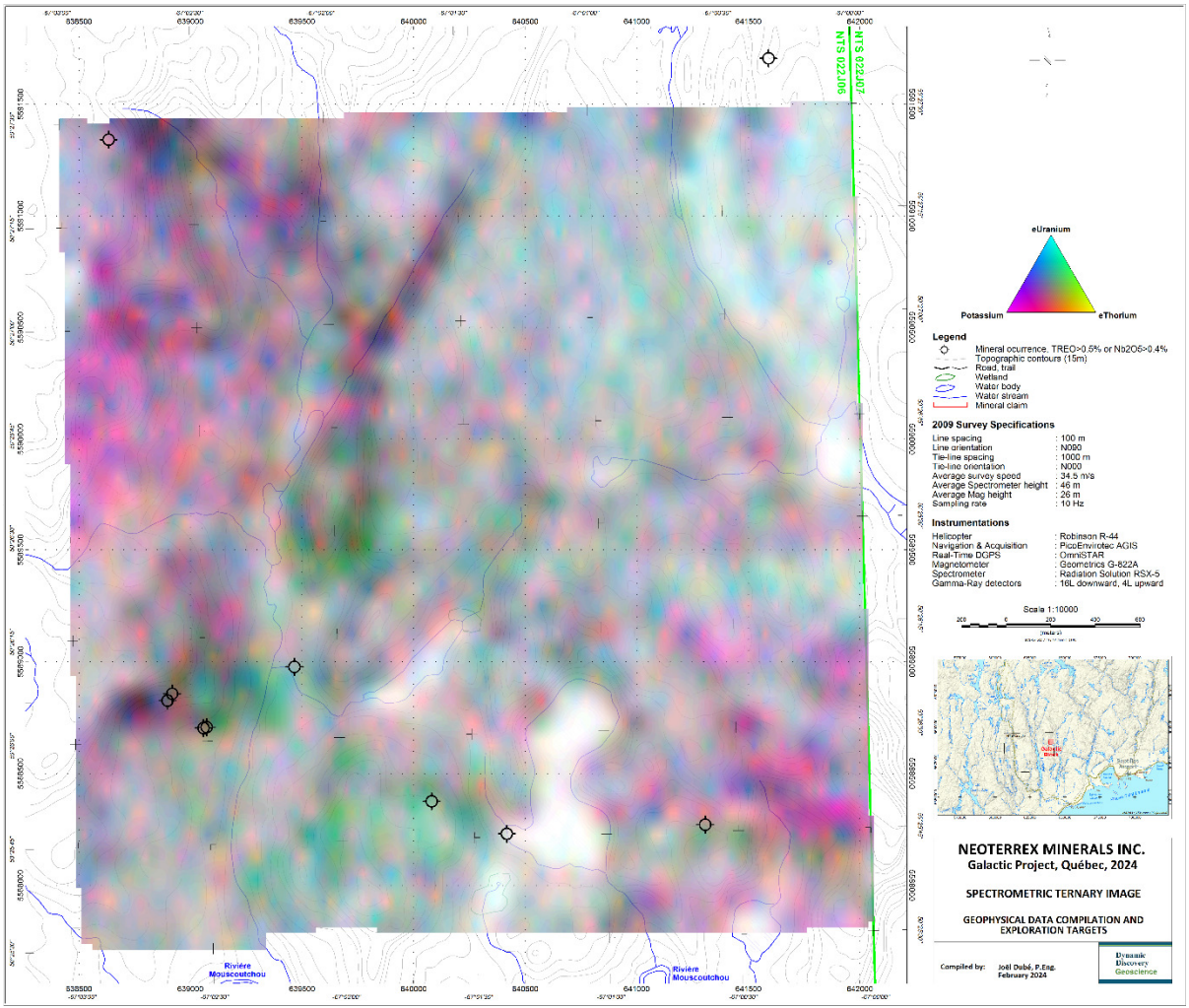

Galactic_INTERPRETATION map

This map shows interpretation and targets defined on the basis of the data compilation results. The possible outlines of interpreted intrusions are highlighted with dashed grey lines. Exploration targets are outlined in dashed burgundy lines, and identified with an ID letter. Note that the targets are not indicated in any specific priority order. Details regarding the interpretation and targets are given in section VI of this report, with explanations regarding the targeting approach. Since the TMI grid is very useful to summarize magnetic structures at a glance, it has been kept in the background of the interpretation map

Figure 13: Galactic area interpretation and exploration targets

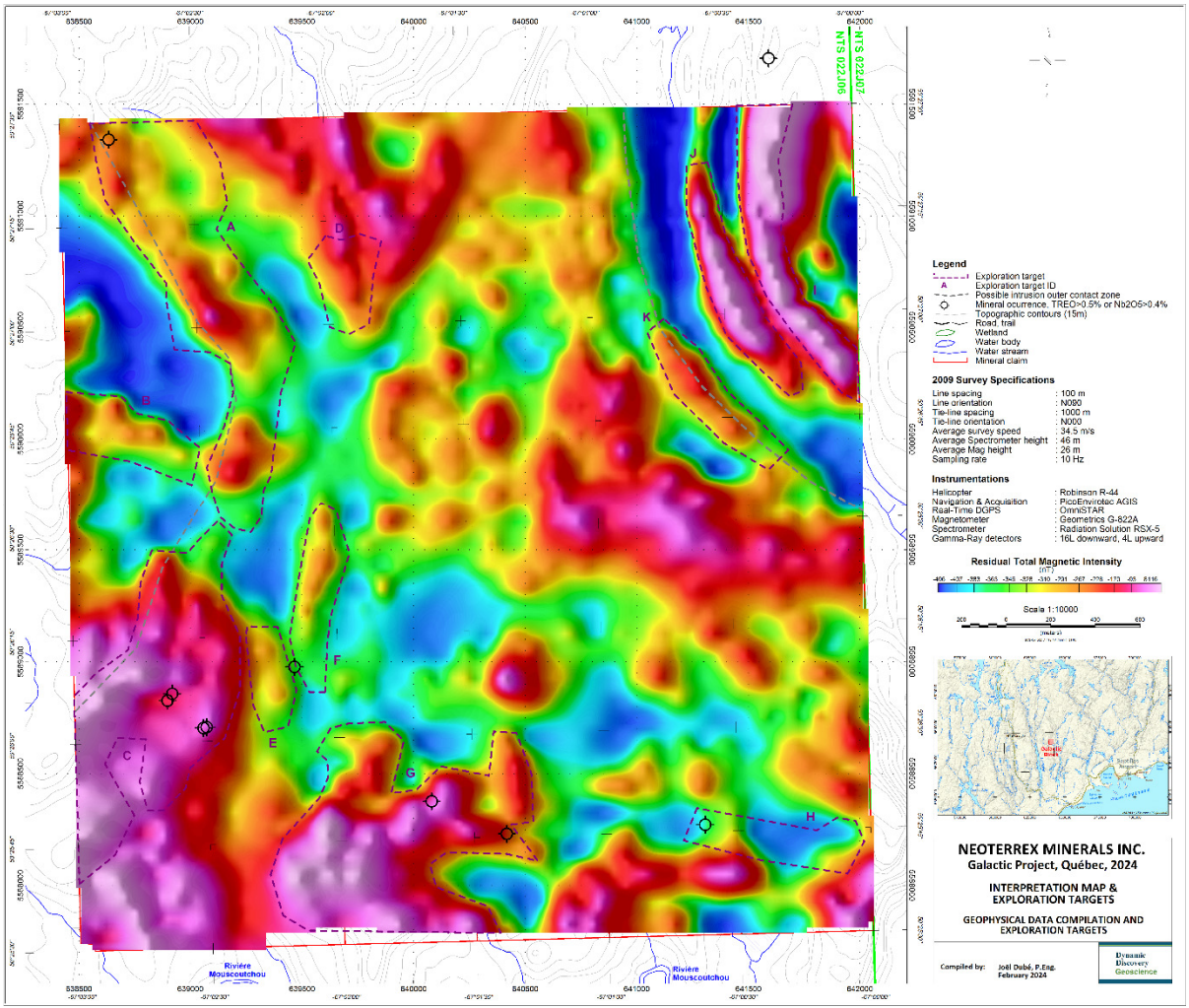

IV. 3D MAGNETIC DATA INVERSION TECHNICAL SPECIFICATIONS

Geophysical data employed

The heliborne magnetic data used for the modelling work are those from the same 2009 survey discussed above, which offer the best resolution for any data set covering the entire Galactic area. The residual total magnetic intensity (TMI) resulting from this survey, shown in Figure 4, was used as the input for the modeling work described below.

Magnetic data inversion

The inversion work was carried out with the VOXI modelling software supplied by Seequent (Geosoft). The inversion algorithms are aimed at creating 3D models of the probable distribution of magnetic susceptibility values within the ground. The output voxel cells size was chosen in accordance with the acquisition parameters thus set to 25m x 25m horizontally (along X and Y axis) and to 10m vertically (along the Z axis), down to the elevation of -40 m, where the Z cell size was then gradually increased with depth. Inversion iterations were carried out until the magnetic data predicted from the model fits the observed data with a maximum error of 3 nT.

The type of magnetic data inversion that was carried out is referred to as Magnetic Vector Inversion (MVI) and takes into account both the induced and remanent magnetization effects. The specifics of the more advanced MVI technique are well described by Geosoft (Ellis et al., 2012 and Macleod et al., 2013). Since remanent magnetization is very common in nature, the MVI results tend to better locate the magnetic sources compared with the standard type of magnetic data inversion, which works with the assumption that only induced magnetism is at play.

The inversion model was created down to the elevation of -850 m, which is equivalent to a depth of about 1 km below the surface's lowest point. However, since shallow model cells are exerting a stronger control over the magnetic data compared with deeper cells, magnetic susceptibility values recovered by the inversion algorithm are considered a lot more accurate near the surface than at depth. Deeper cells are mostly controlling long wavelength anomalies. Considering this, the final model is deemed reliable only for the first few hundred meters closer to surface.

The Galactic final model voxel size is of 146x152x137 cells (in X, Y, and Z directions).

3D Magnetic Data Inversion Presentation

The 3D model of MVI susceptibility is presented in different ways. First of all, it is presented as 3D images. Figures 14 and 15 show the magnetic 3D model with a plunging view looking north and east, respectively. Iso-surfaces of 4.1, 6.4, 8.0 and 13.4 mSI are shown. Plan view maps of the results extracted as horizontal slices at 50, 100 and 200 m depth were also created. They are presented individually on maps shown on Figures 16 to 18.

Figure 14: 3D view of the MVI susceptibility model, looking north

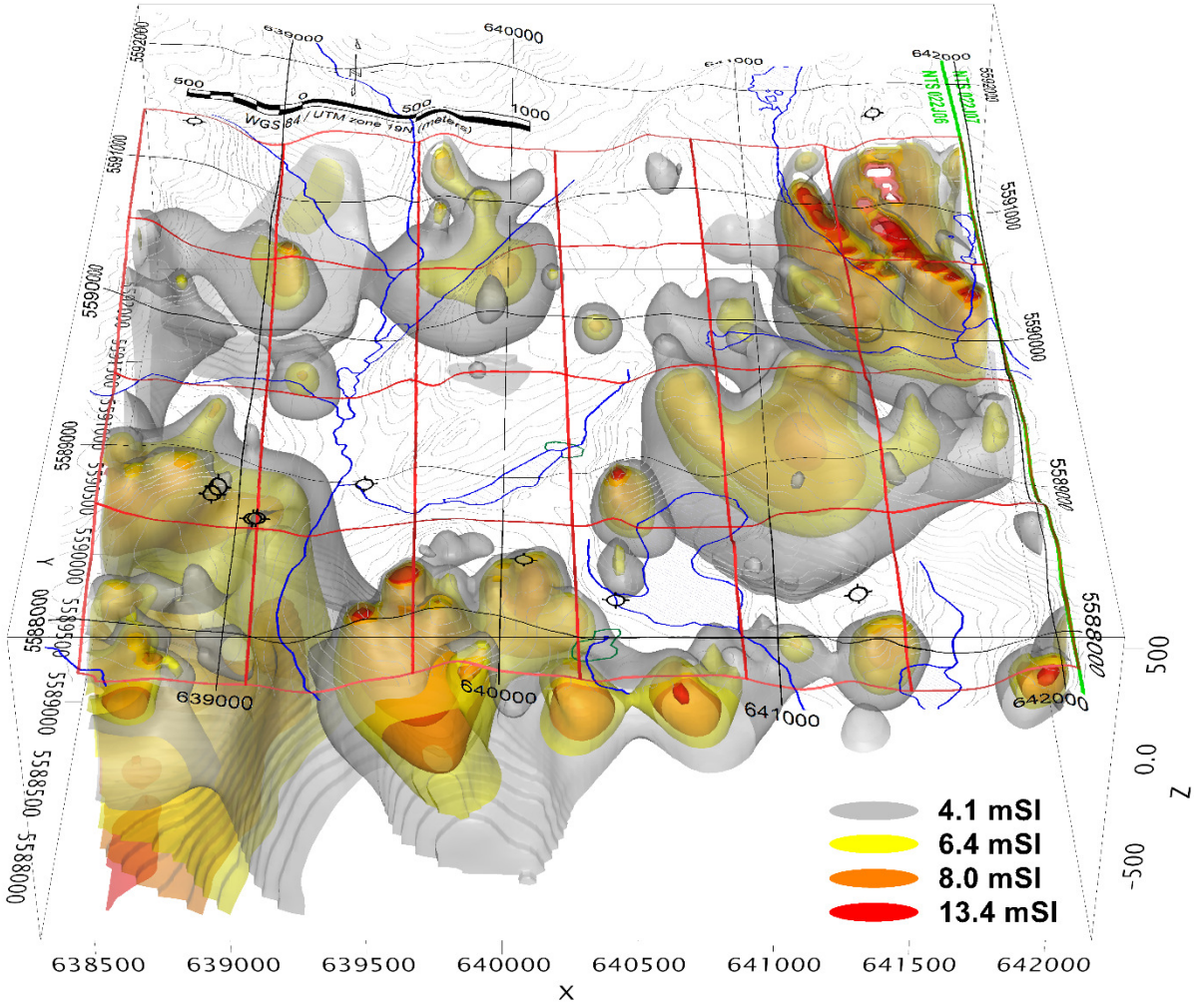

Figure 15: 3D view of the MVI susceptibility model, looking east

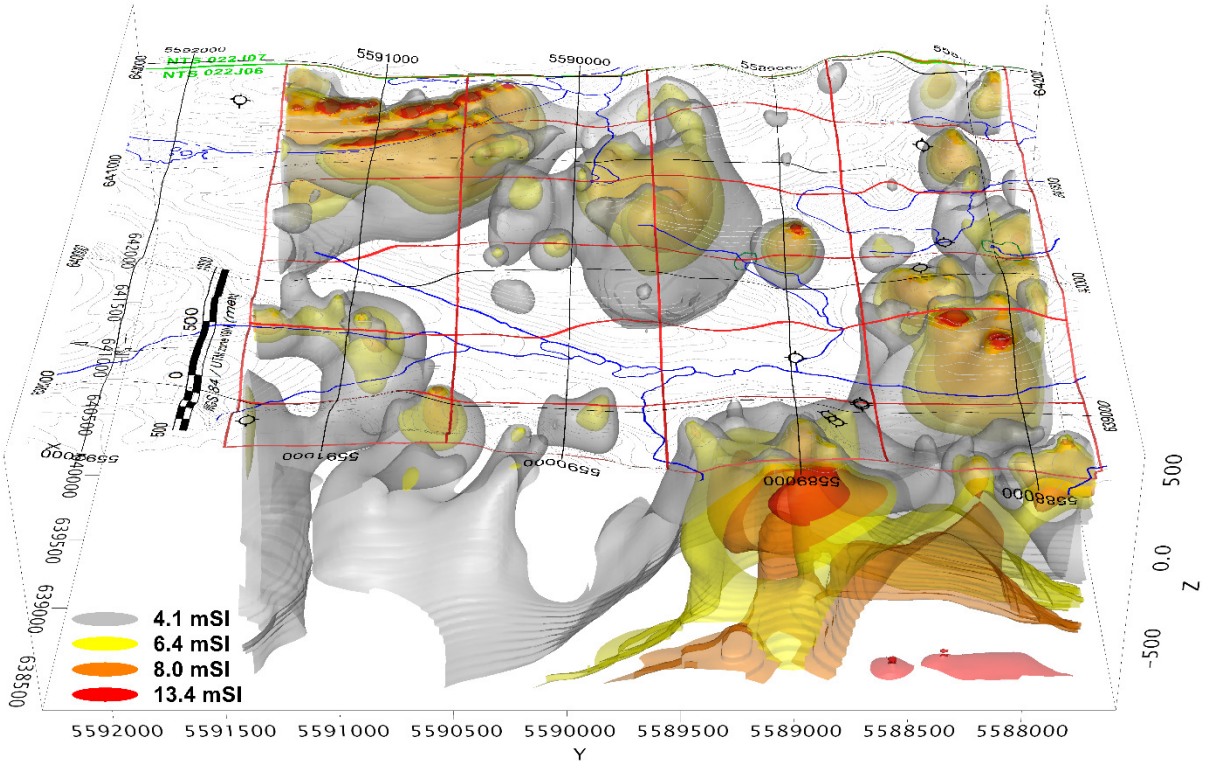

Figure 16: MVI susceptibility model sliced at 50m depth

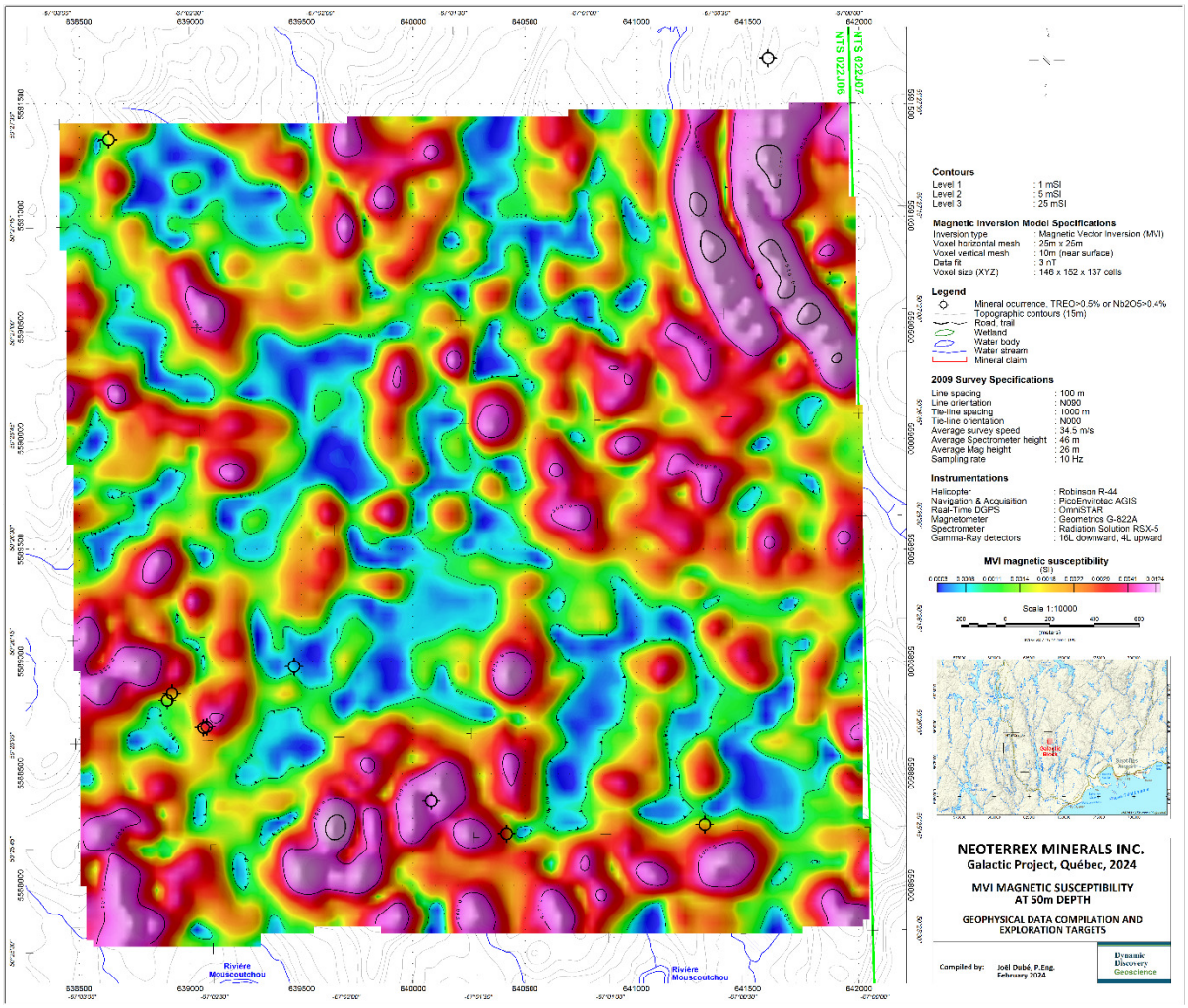

Figure 17: MVI susceptibility model sliced at 100m depth

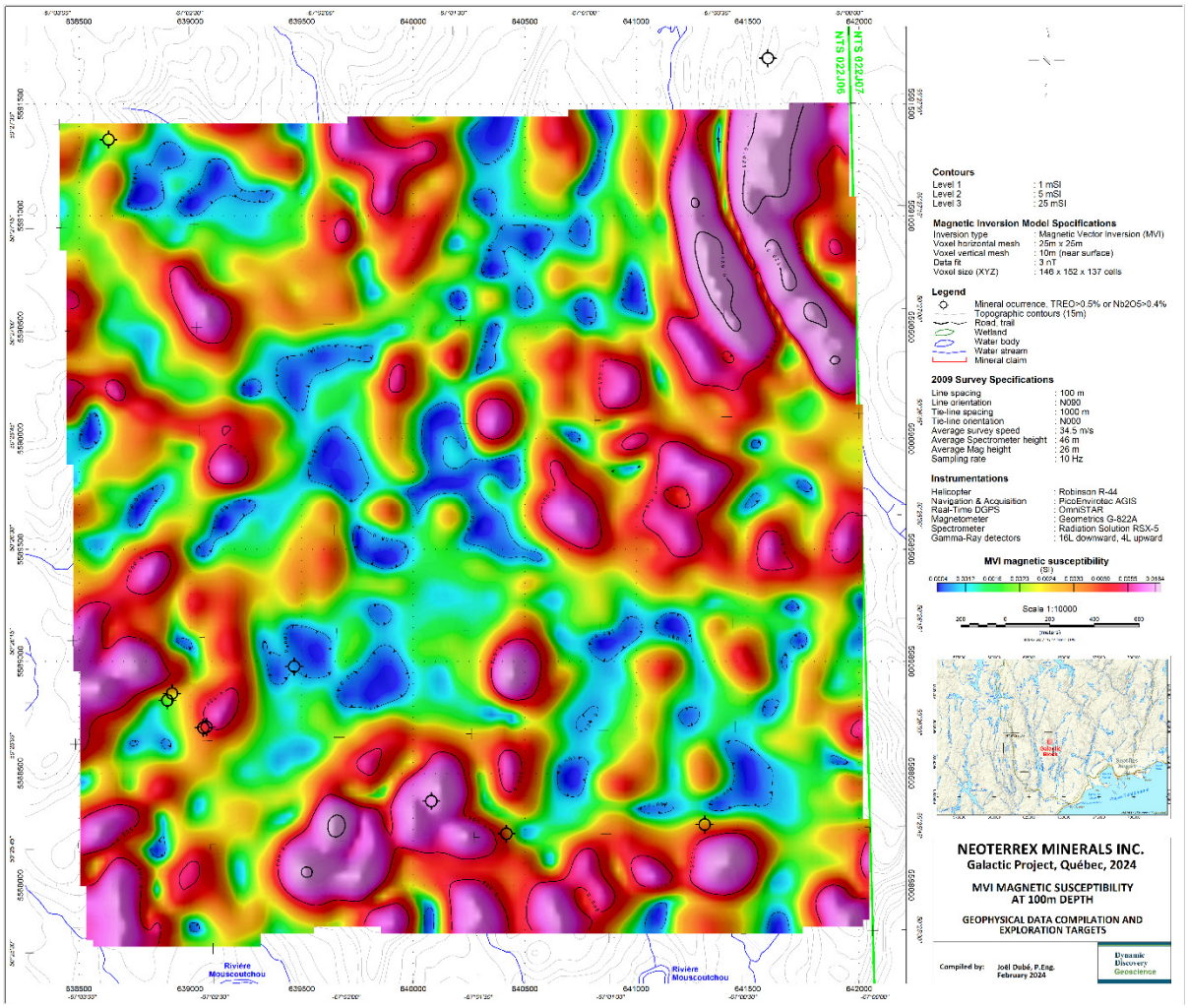

Figure 18: MVI susceptibility model sliced at 200m depth

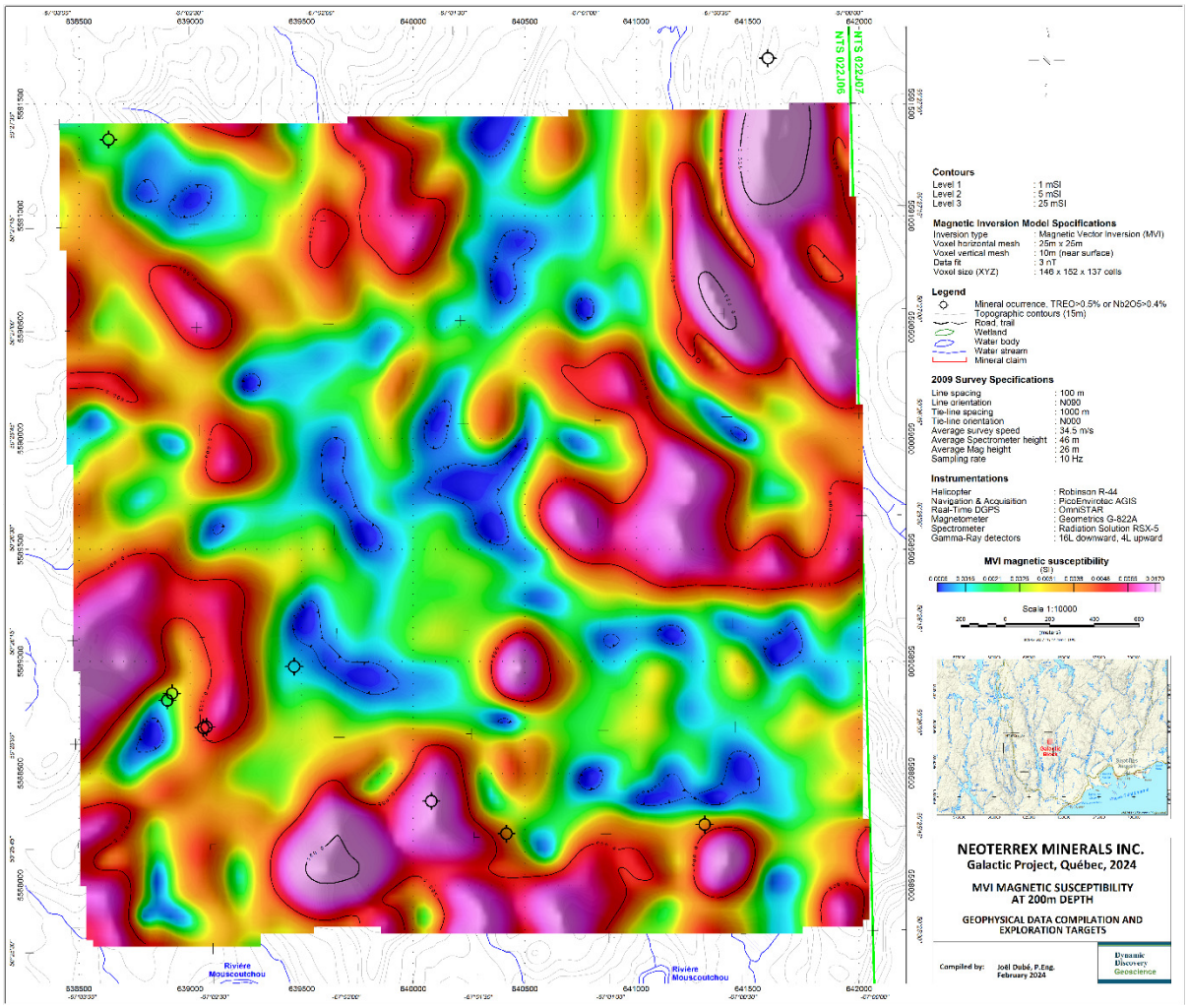

V. DELIVERABLES

Deliverables

The maps described above and delivered as part of this work are listed in Table 1. All maps are referred to WGS-84 in the UTM projection Zone 19 North, with coordinates in metres. Maps are at a 1:10,000 scale and are provided in PDF, PNG, GeoTiff and Geosoft MAP formats.

Table 2: Delivered maps

No.	Nom	Description
1	DEM+FlightPath+Claims	Digital Elevation Model with flight path and Property claims
2	TMI	Residual Total Magnetic Intensity
3	FVD	First vertical derivative of the TMI
4	TILT	Tilt Angle Derivative
5	Total_Count	Gamma-ray total count
6	Potassium	Potassium concentration
7	eUranium	Equivalent Uranium concentration
8	eThorium	Equivalent Thorium concentration
9	Ternary_Spectro	Spectrometric ternary image
10	Ratio_eTh-K	Equivalent Thorium/Potassium ratio
11	MVIsusceptibility_50m	MVI magnetic susceptibility at 50m depth
12	MVIsusceptibility_100m	MVI magnetic susceptibility at 100m depth
13	MVIsusceptibility_200m	MVI magnetic susceptibility at 200m depth
14	INTERPRETATION	Interpretation map

VI. DATA INTERPRETATION AND EXPLORATION TARGETS

General interpretation and targeting approach

The residual Total Magnetic Intensity (TMI) of the Galactic block, presented in Figure 22, is slightly active and varies over a range of 1,519 nT, with an average of -258 nT and a standard deviation of 159 nT. The magnetic textures and relatively low amplitude signal variations seen throughout the block are typical of felsic to intermediate intrusive rocks, with meta-sedimentary rocks occurrences also considered possible locally. Weak magnetic anomalies, occurring either in compact or linear shapes, are related to slight concentrations of pyrrhotite or magnetite. Stronger anomalies are best seen on Figure 23 which shows the residual TMI data with a linear color distribution. Note however that these stronger anomalies are actually very weak in absolute terms.

There are two most prominent magnetic features found in the area. Both are associated to sizable magnetic anomalies consisting of intertwined magnetic highs and lows, indicating that remanent magnetism may affect them, and interpreted to originate from intrusive bodies of different composition than most surrounding host rocks. Because these features are large and mostly found outside of the survey block, they are easier to see on the regional magnetic data from the 2017 fixed-wing survey reported by Québec's MERN

(Vallières et al., 2017). These regional data are shown on Figures 19 and 20 and the possible outlines of the two inferred intrusions are also indicated on these figures.

Figure 19: Regional TMI data with Galactic claims and interpreted intrusions

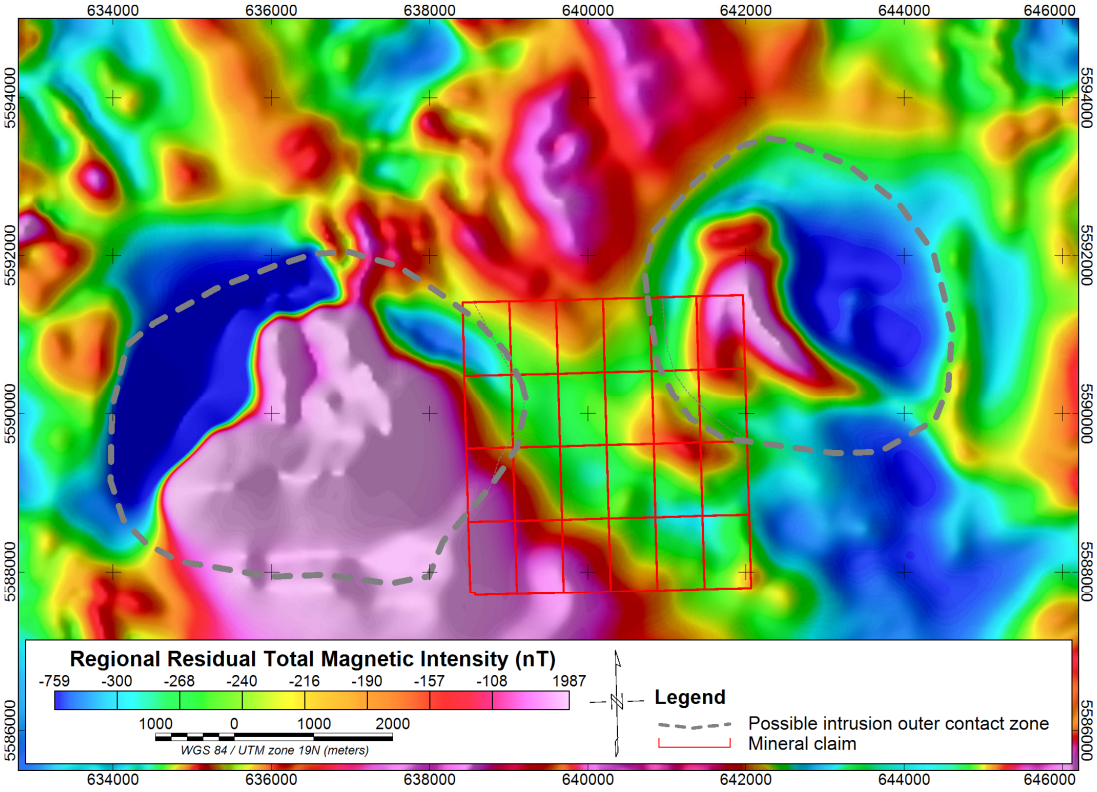

Figure 20: Regional FVD data with Galactic claims and interpreted intrusions

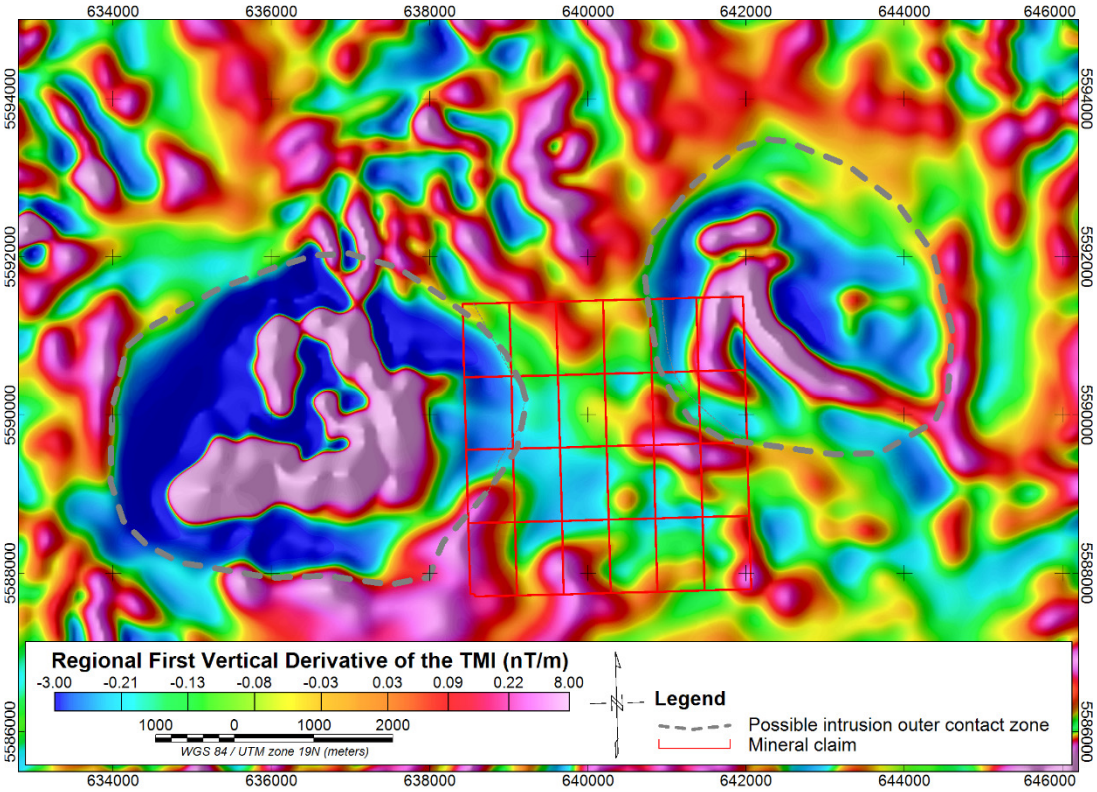

Given the low resolution from the 2017 fixed-wing airborne survey, the 2009 heliborne survey data allow for more detailed interpretation and so a refined version of the possible intrusions' outer contact zones is indicated on all the other figures of the report.

The intrusion located on the west side of the block has a significantly magnetic core zone (outside of the survey block) surrounded by a relatively low magnetic area, which is finally bordered by a weak magnetic lineament interpreted to indicate the possible contact zone of the intrusion. This contact zone happens to lie at the eastern limit of a wide topographic high. This zone is also characterized by stronger radiometric values in general. It is very interesting to note that 6 of the 10 occurrences mineralized in REE found in the area are located within 1 km of this inferred contact zone. Radiometric responses are also mostly strong in areas nearby this interpreted contact zone, which can be seen on the gamma-ray total count product.

On the other hand, the possible intrusion found at the northeast corner of the block has a less magnetic core zone (outside of the survey block), and rather depicts concentric magnetic lineaments possibly indicating internal structures of the intrusion. It is also located within a relatively low radiometric background area. This inferred intrusion has no clear correlation to topographic data, except for the narrow magnetic lineaments which are coincident with subtle topographic highs. One REE mineralized occurrence is found near this interpreted contact zone, to the north of the survey block.

Another difference between the two outlined possible intrusions is that the less magnetic part of the west intrusion depicts enrichment in Potassium over eThorium and eUranium (as can be seen on the various radio-elements ratios and the spectrometric ternary image), while the northeast intrusion rather appears with slightly higher eUranium, and to a lesser extent eThorium, values relative to Potassium amplitudes.

Given their very different geophysical and topographical signatures, both interpreted intrusions are believed to be of different nature and composition. It is however possible that both could have played a role in the genesis of the REE mineralization sought after, such as by having served as the magmatic sources for the later differentiated and fractionated pegmatites emplaced in the area. These harder to deform intrusions may also have caused pressure shadow areas and brittle structures to develop in their vicinity, which could have enabled the emplacement of mineralizing hydrothermal systems.

When looking at the location of REE mineralized occurrences in conjunction with geophysical results, it is seen that most (8 out of 10, if we include the northernmost occurrence located outside of the survey block, but in direct continuity with the strongest magnetic lineament of the northeast postulated intrusion) are directly associated, or found very close, to magnetic anomalies of different amplitudes. A few of the mineralized occurrences have been shown to be associated with magnetite to some degree, which would explain these results. The majority of mineralized occurrences are also associated with radiometric anomalies ranging from weak to strong, as seen on the total count results, and also on the eUranium and eThorium values and their ratios, which is also expected given the common association between REE mineralization and these radio-elements

Based on these observation and principles, a number of focussed exploration targets, or prospective areas, have been defined using the geophysical data to guide exploration efforts. Prospective areas are outlined as thick dashed burgundy lines on the interpretation map. They are also shown on Figures 21 to 34 which put each target in the context of its geophysical responses as reflected in each data set part of the compilation and 3D modelling work. Each of these exploration targets was identified with a letter (from A to K), which does not relate to any specific priority order. In total, 11 targets have been identified. They are briefly described in the following section.

Galactic Property targets

Details about each exploration targets are provided here.

Targets A, B and C are located in the vicinity of the postulated west intrusion's contact zone outline where several REE mineralized occurrences have been discovered. While Targets A and C are more or less following this possible contact zone, along with distinctive magnetic lineaments parallel to it and fairly strong gamma-ray total count, eUranium and eThorium anomalies, Target B rather focuses on a magnetic lineament radial to the intrusions' mass center, which could relate to a fracture with presence of some magnetite, and where a weak total count and Potassium anomaly is found.

Target D is focussing on the south tip of a 'V' shaped magnetic anomaly which could relate to a fold hinge, in an area where total count, eUranium and eThorium values are particularly high, especially considering the fact that this area depicts relatively flat topography compared to other radiometric anomalies of the same amplitude but that are coincident with sharp cliffs, valleys or topographic changes. Here it should be noted that areas with sharp topographic changes tend to have more outcropping rocks, with minimal overburden or vegetation on top, and also imply ground surface geometries which expose the spectrometer on-board the helicopter to gamma-rays not only coming from the ground below the helicopter, but also from the rocks to the sides, artificially increasing radiometric values compared to flying the same geology over a flat topography.

Targets E and F pertain to two distinct N-S trending and narrow magnetic lineaments found on either side of a known REE occurrence. They are also covering interesting eUranium and eThorium anomalies, which are also seen on the eTh/K ratio, and to a lesser extent on the eU/K ratio.

Target G encompasses two REE mineralized occurrences and some hills characterised by decent magnetic anomalies, as well as radiometric anomalies manifesting themselves in the eUranium and eThorium spectrum, and on their ratios relative to Potassium.

Target H includes another REE mineralized occurrence found beside a very marginal magnetic anomaly, and is mostly of interest on the basis of its eUranium and eThorium radiometric anomalies.

Note that for Targets E, F, G and H, the higher concentrations in eUranium and eThorium can also been seen as green colours on the spectrometric ternary image.

Targets I, J and K relate to three magnetic lineaments concentric to the northeast intrusion and correlated to low amplitude topographic highs. Target I locally hosts the strongest magnetic value of the survey block and is in the direct southern extension of a REE occurrence found about 220 m further to the north, outside of the Property. A small area at the north end of this Target also depicts a radiometric anomaly in total count, eUranium and eThorium. Target J contains radiometric anomalies with higher ratios values in eTh/K and eU/K, within its northern half. The magnetic lineament at Target K is of weaker amplitude. A weak total count anomaly is also found at the southeast tip of the Target.

Figure 21: Exploration targets and DEM data

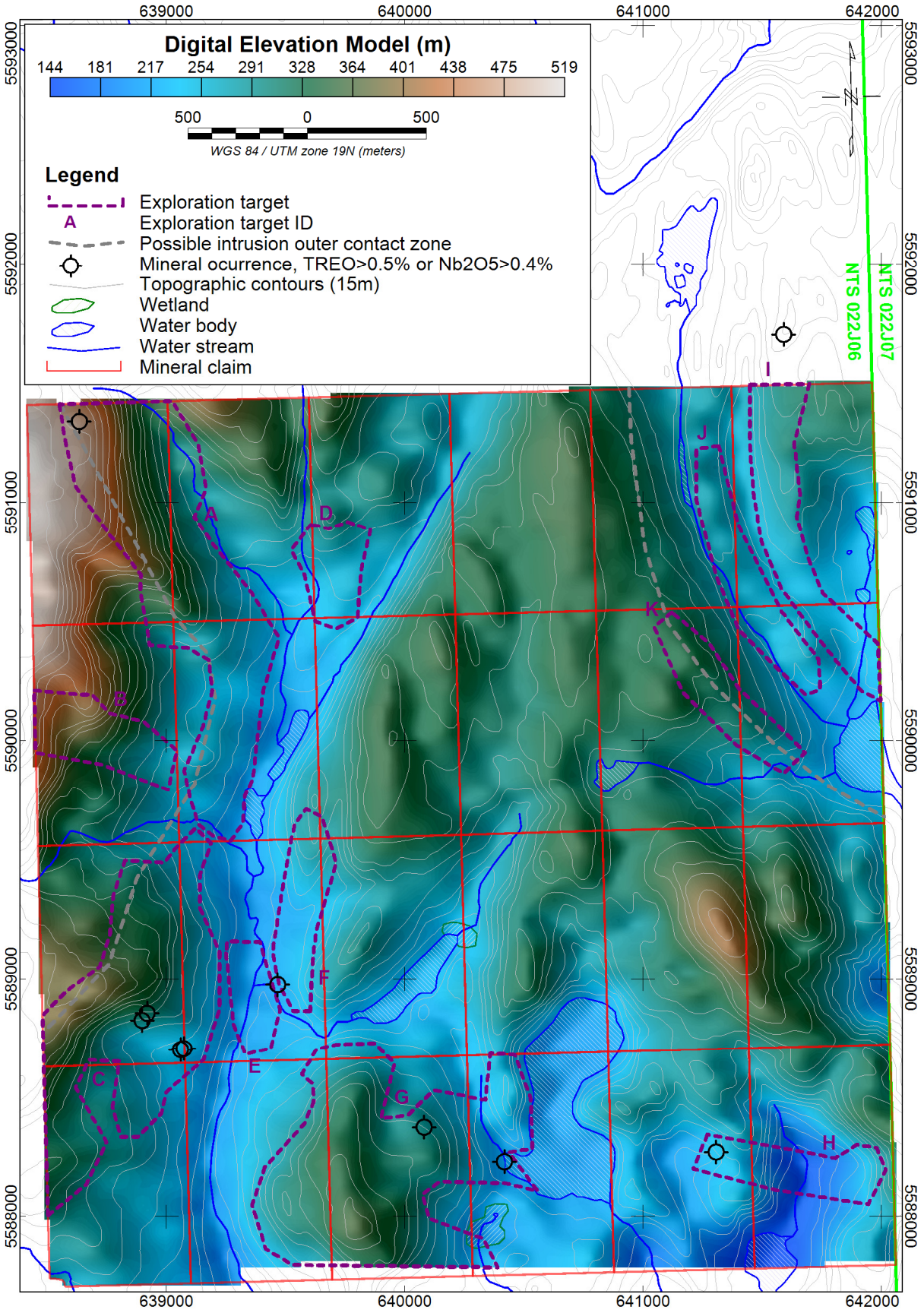

Figure 22: Exploration targets and TMI data with equal area color distribution

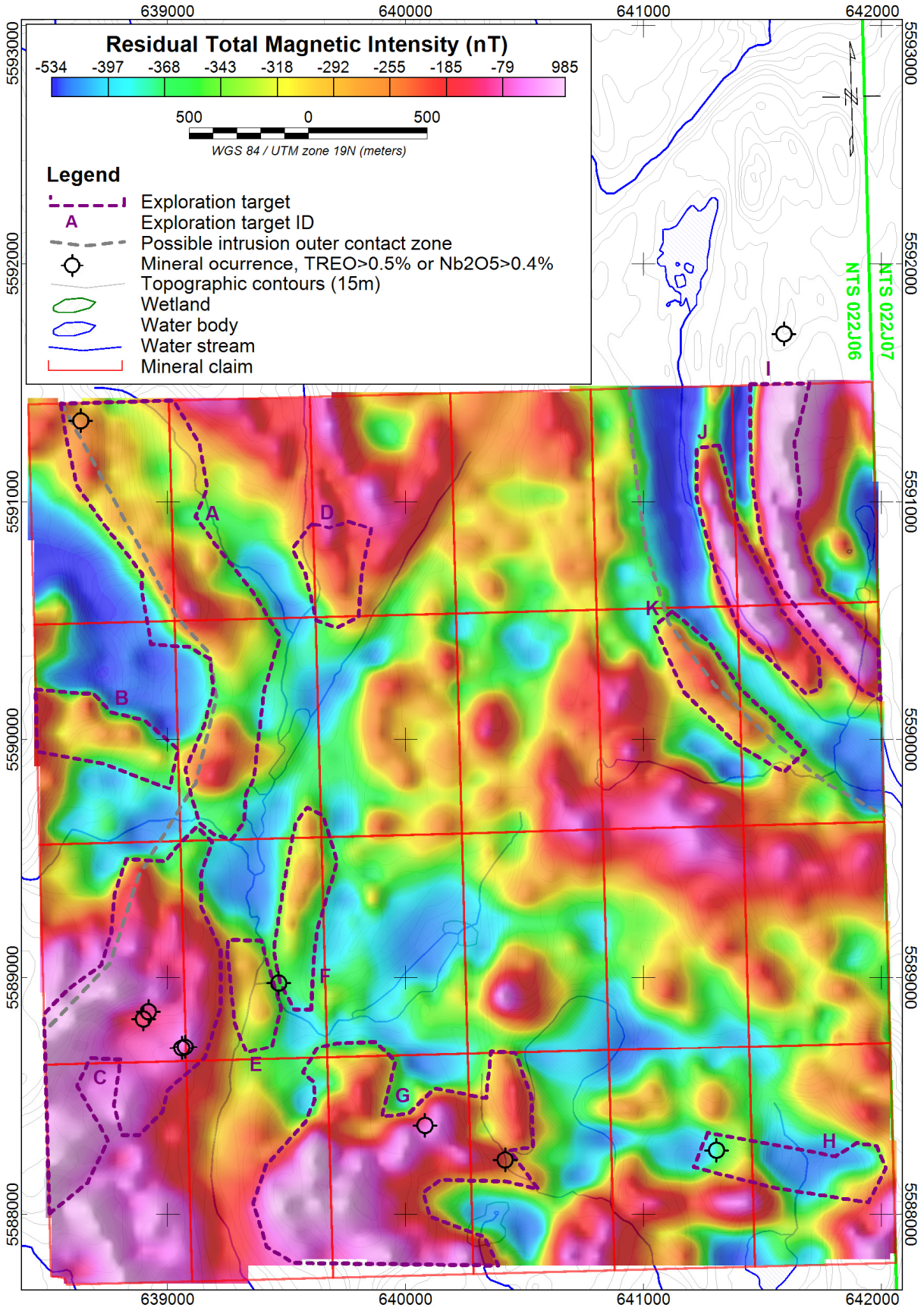

Figure 23: Exploration targets and TMI data with linear color distribution

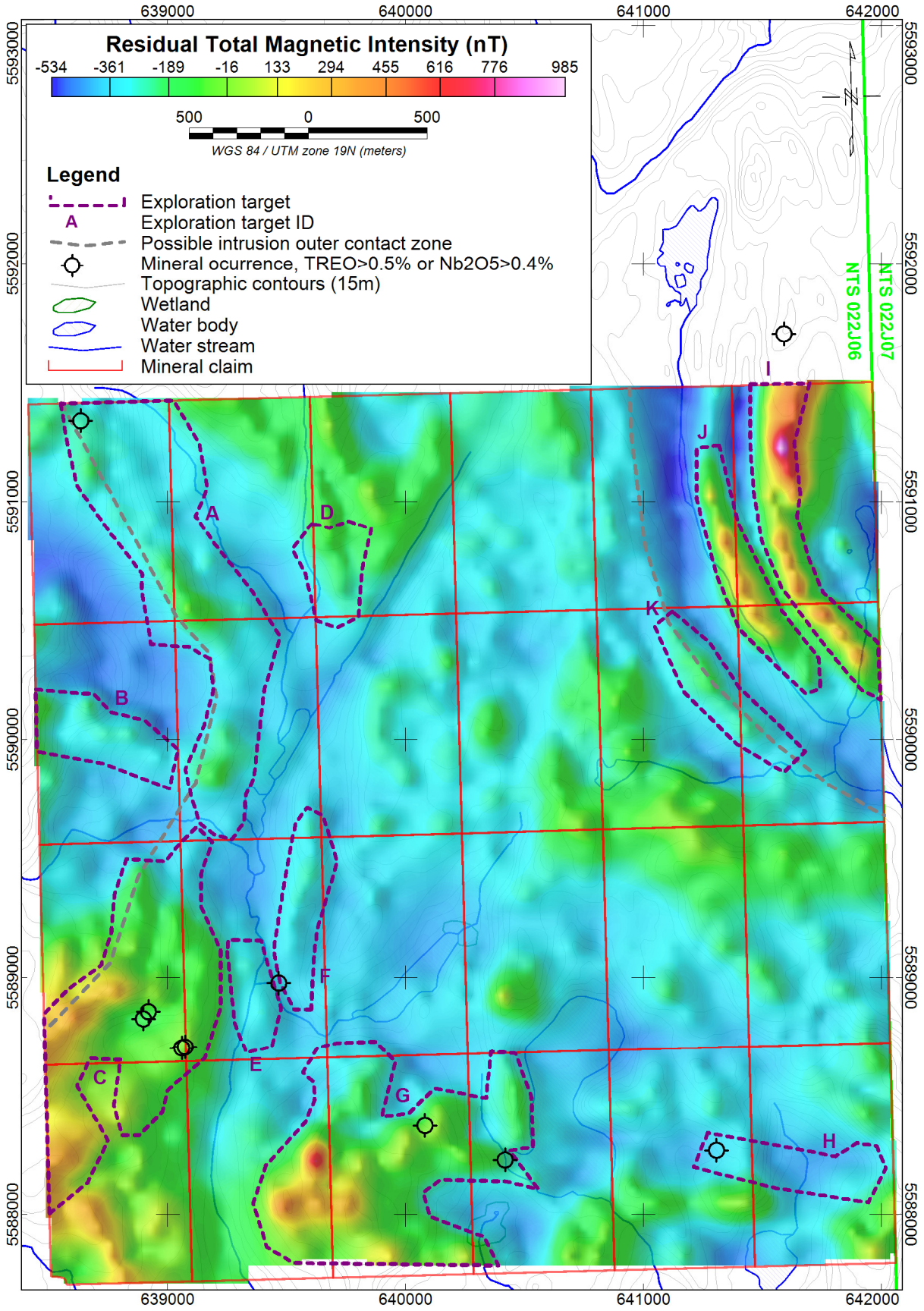

Figure 24: Exploration targets and FVD data

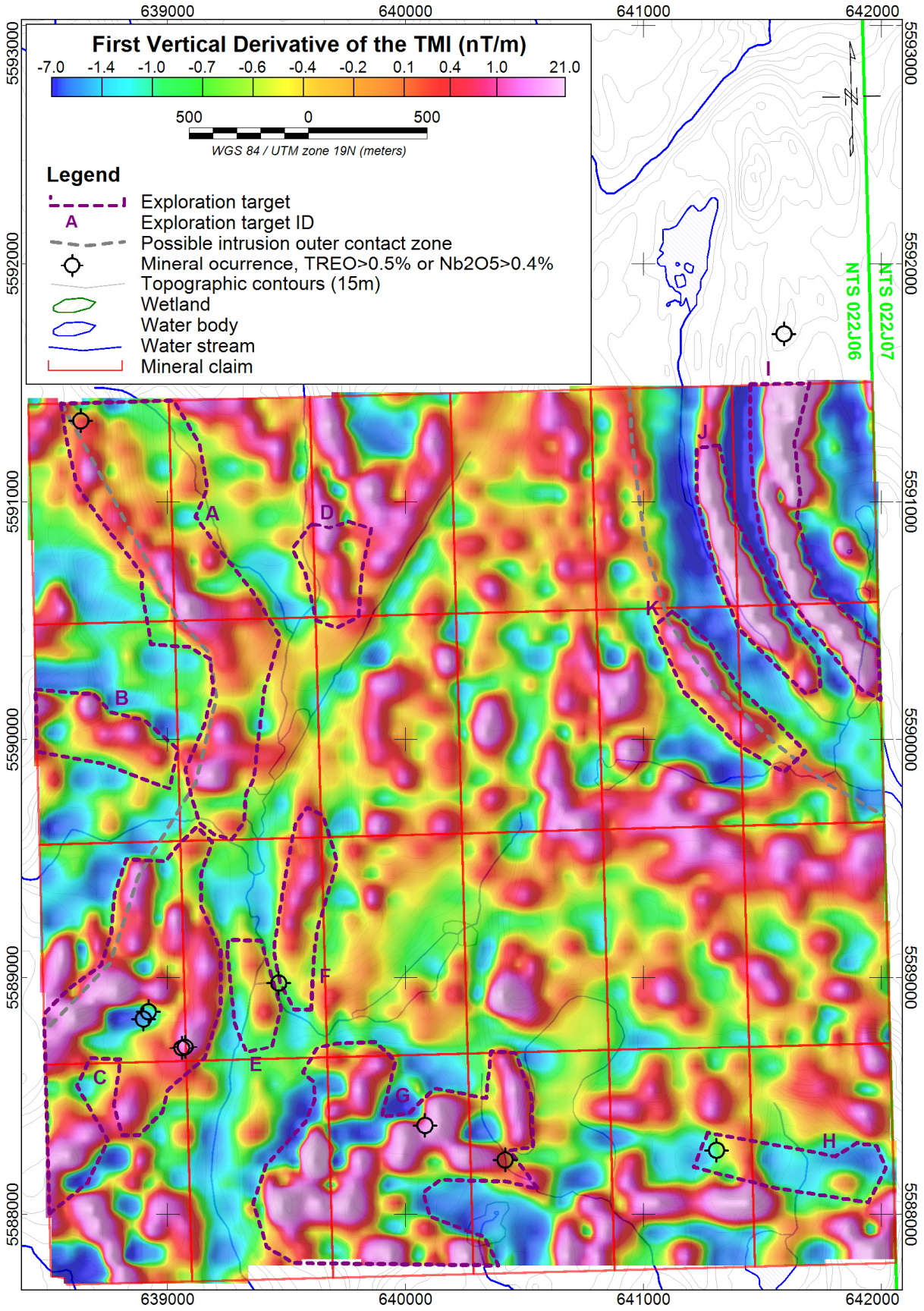

Figure 25: Exploration targets and TILT data

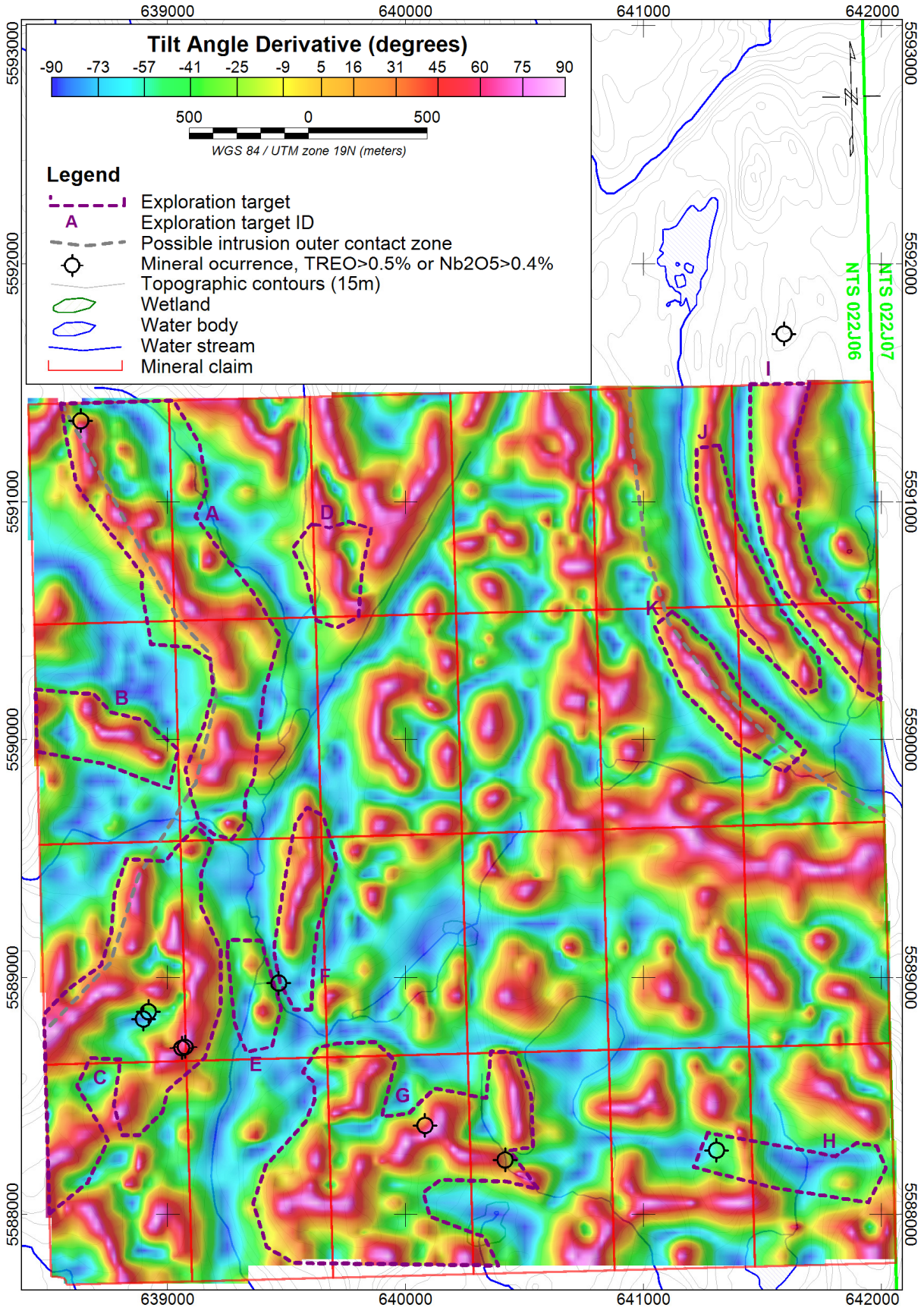

Figure 26: Exploration targets and gamma-ray total count data

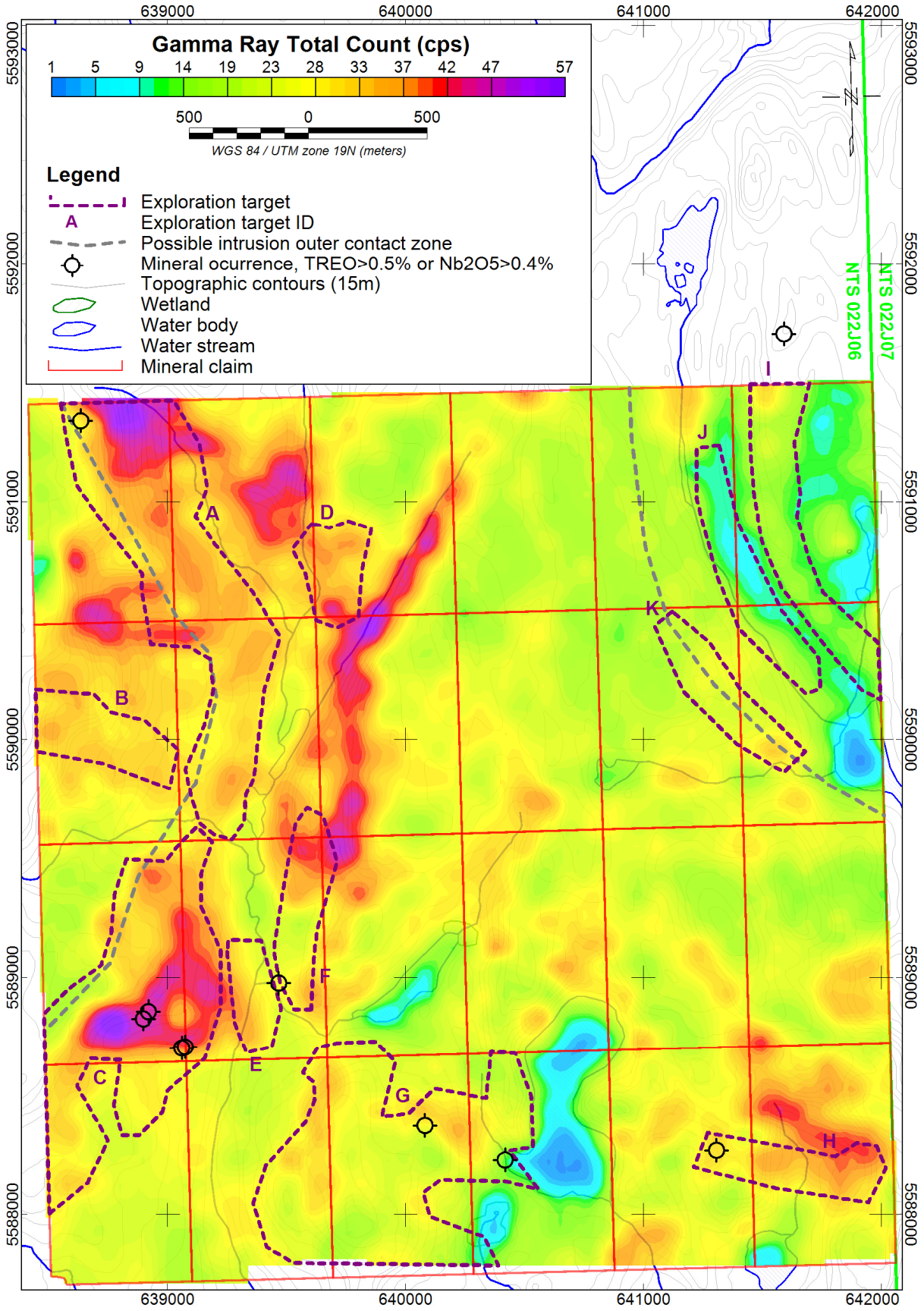

Figure 27: Exploration targets and Potassium concentration data

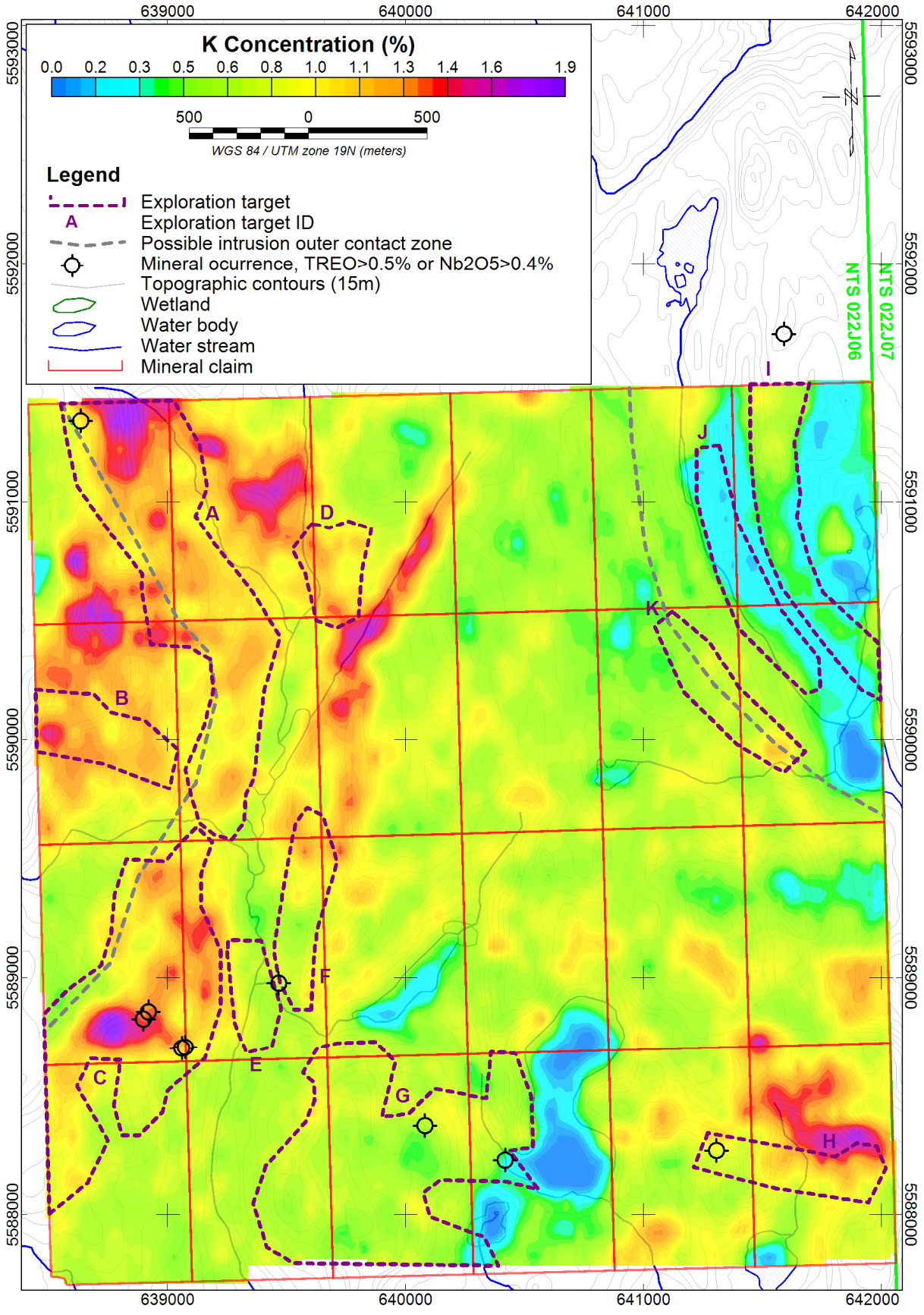

Figure 28: Exploration targets and equivalent Uranium concentration data

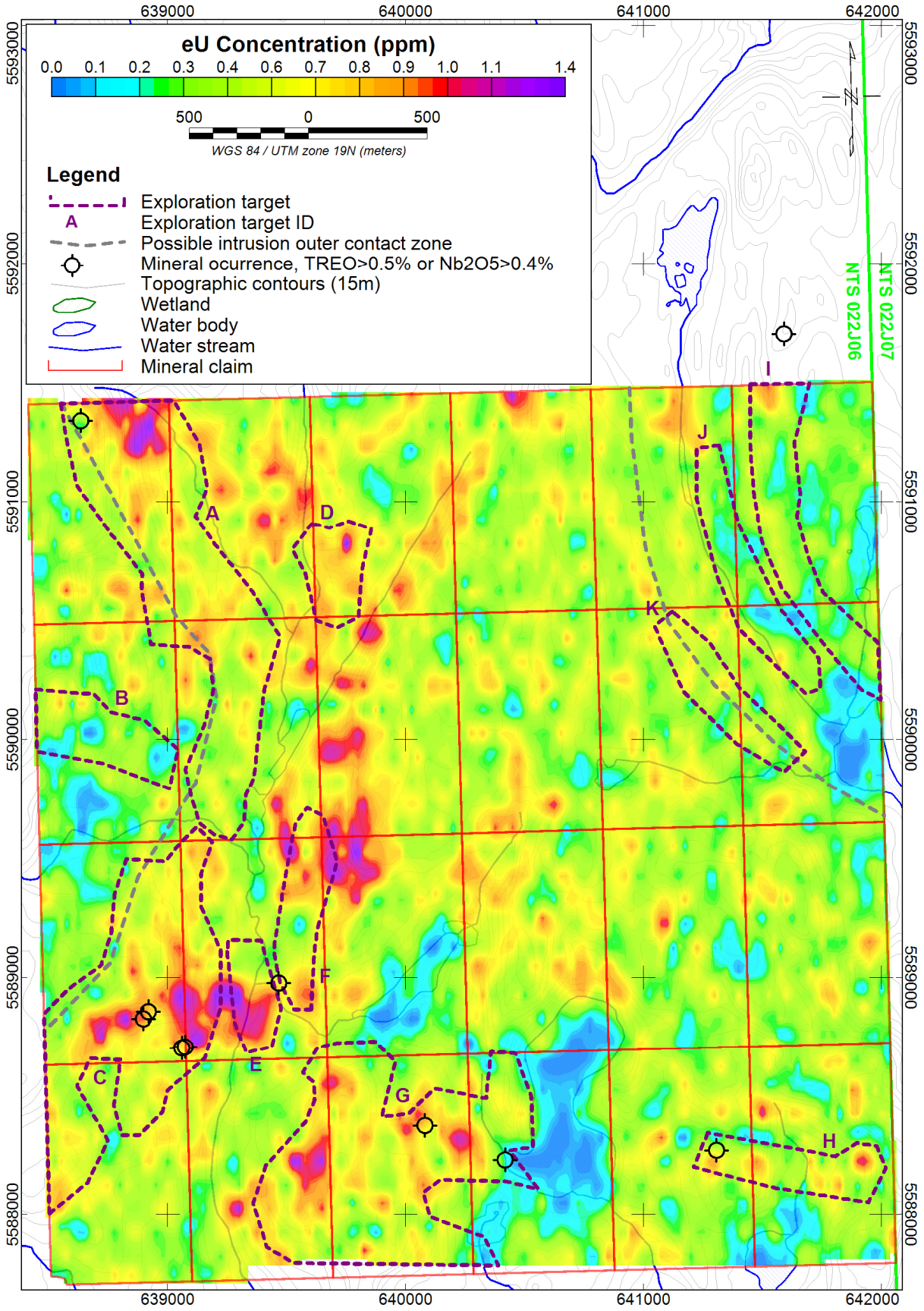

Figure 29: Exploration targets and equivalent Thorium concentration data

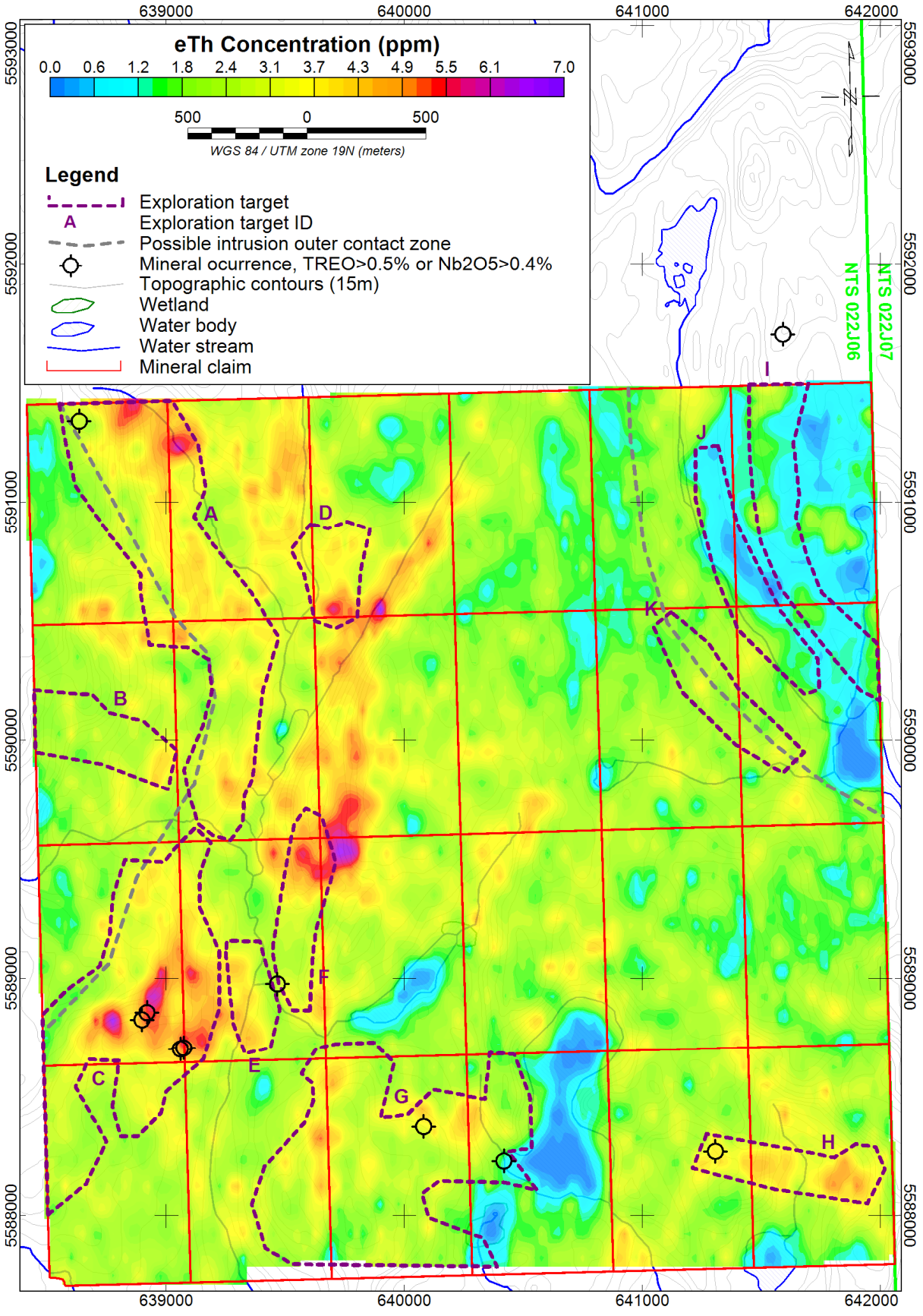

Figure 30: Exploration targets and Thorium/Potassium ratio data

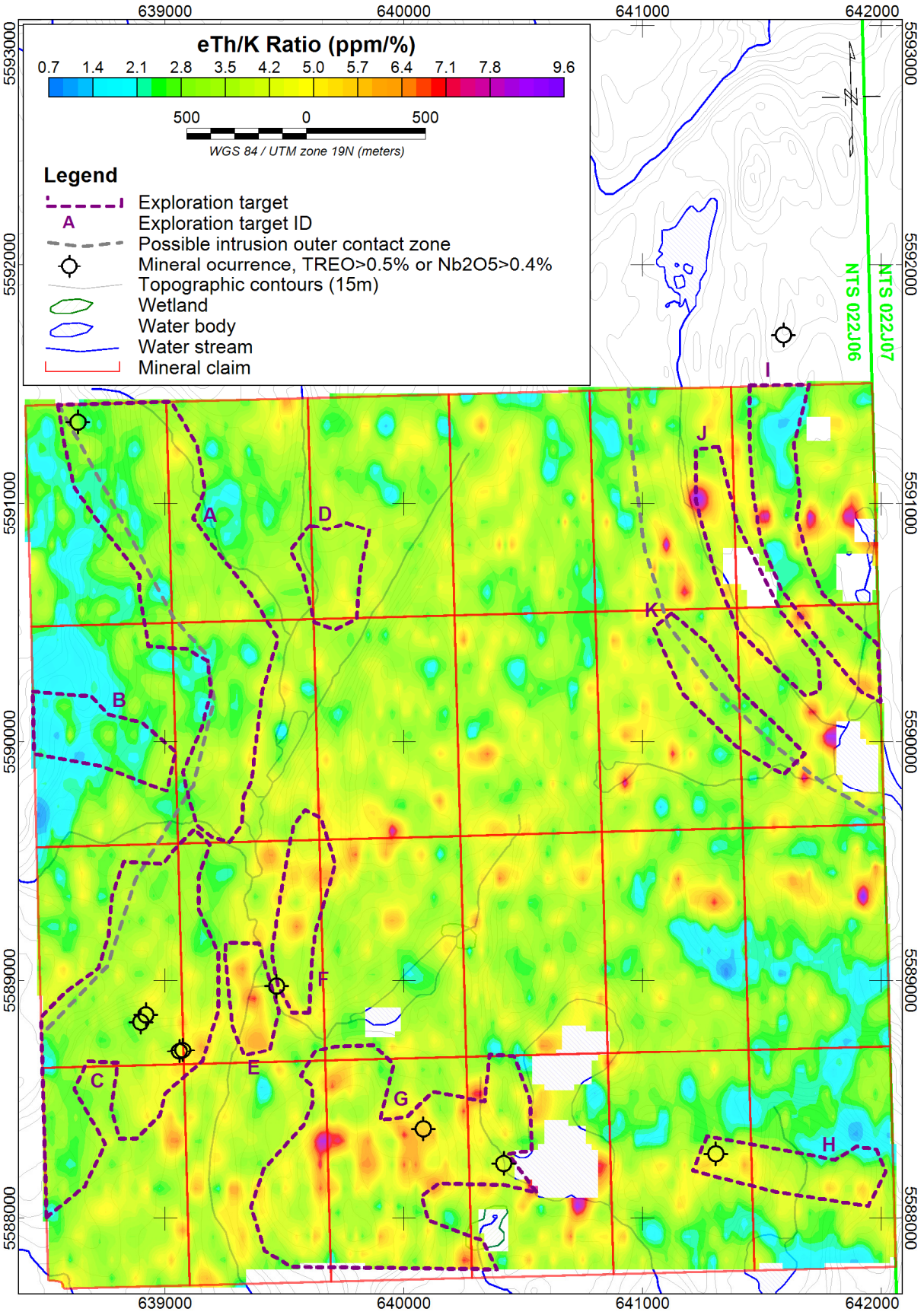

Figure 31: Exploration targets and spectrometric ternary image data

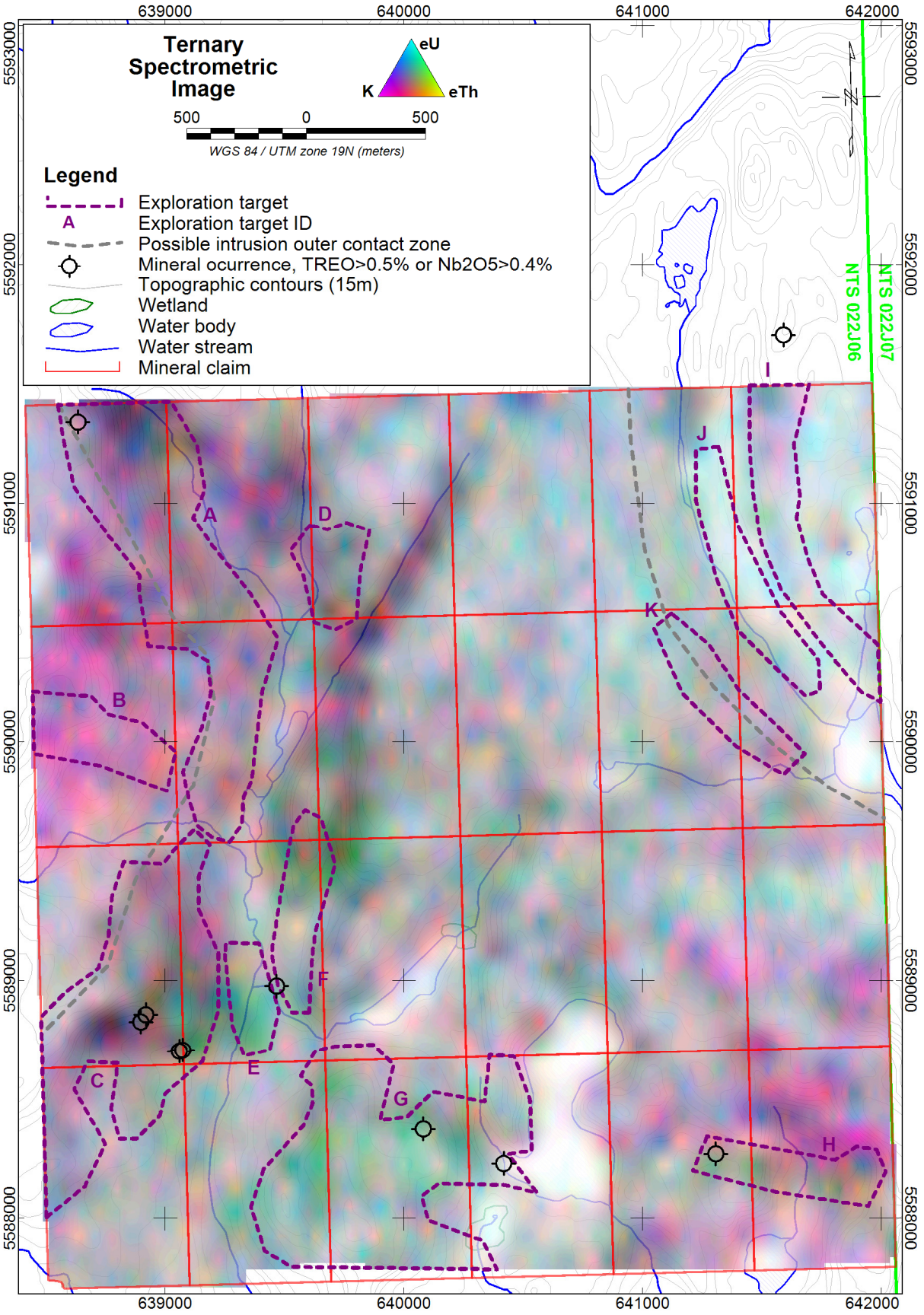

Figure 32: Exploration targets and MVI susceptibility model data sliced at 50m depth

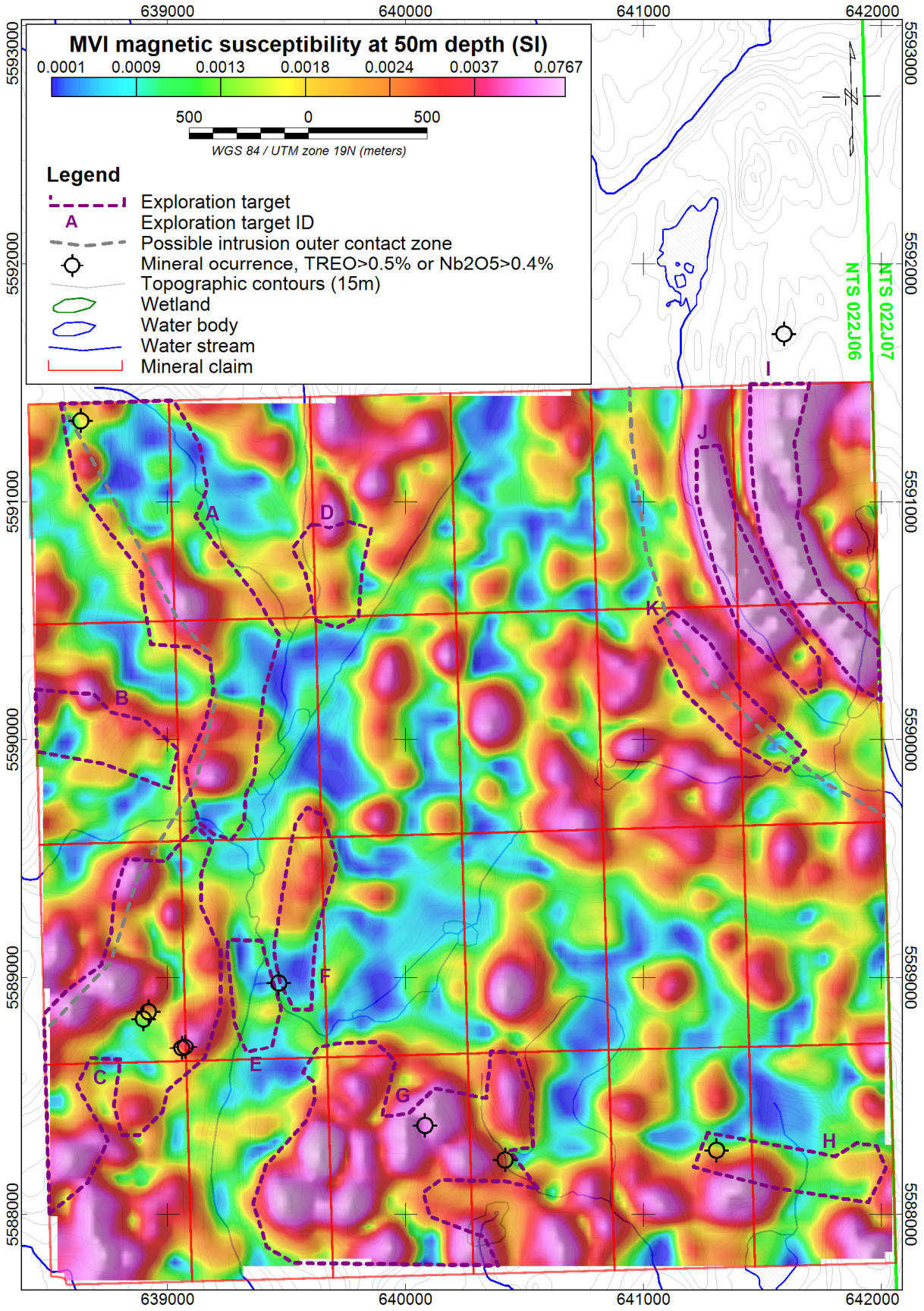

Figure 33: Exploration targets and MVI susceptibility model data sliced at 100m depth

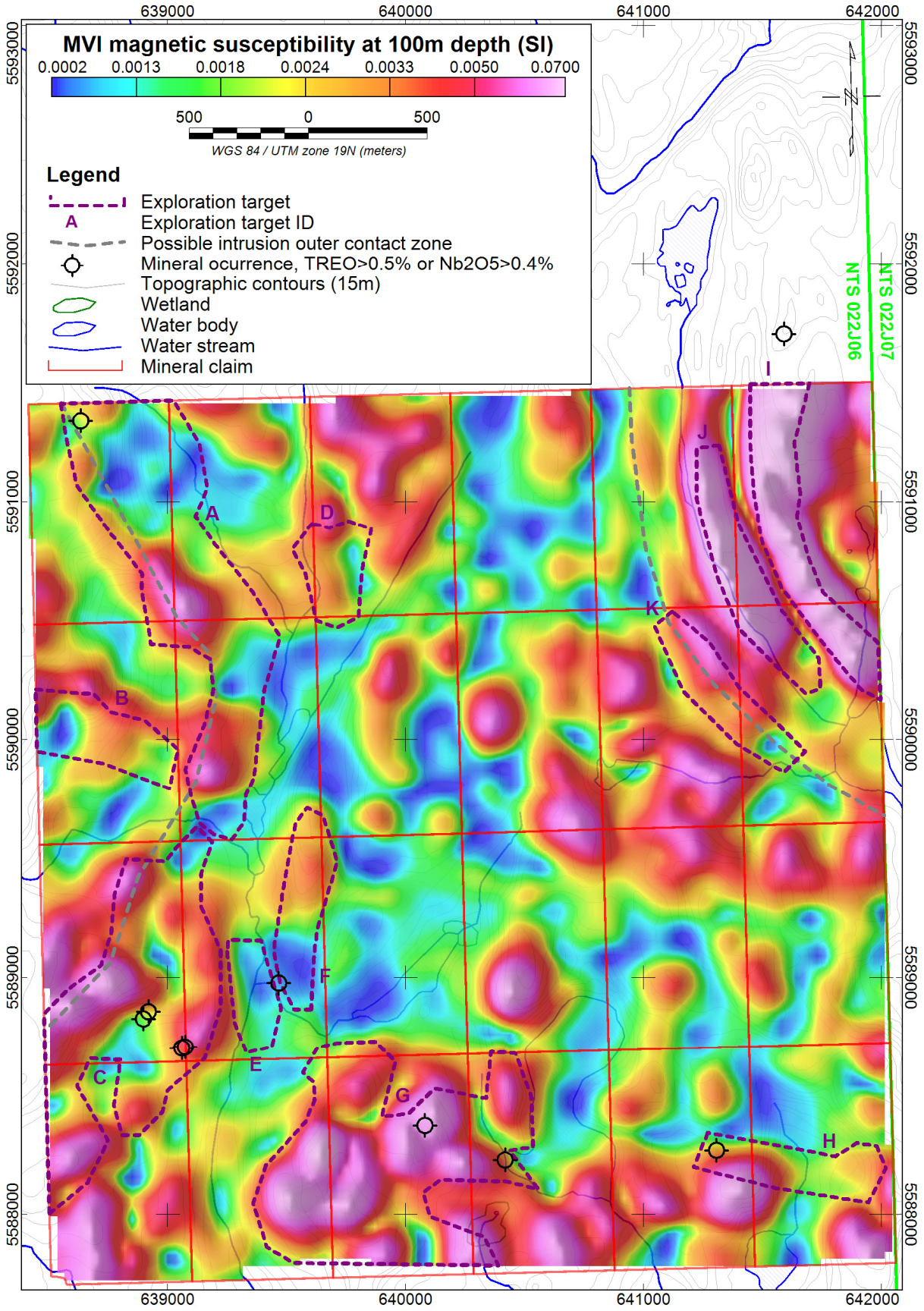

Figure 34: Exploration targets and MVI susceptibility model data sliced at 200m depth

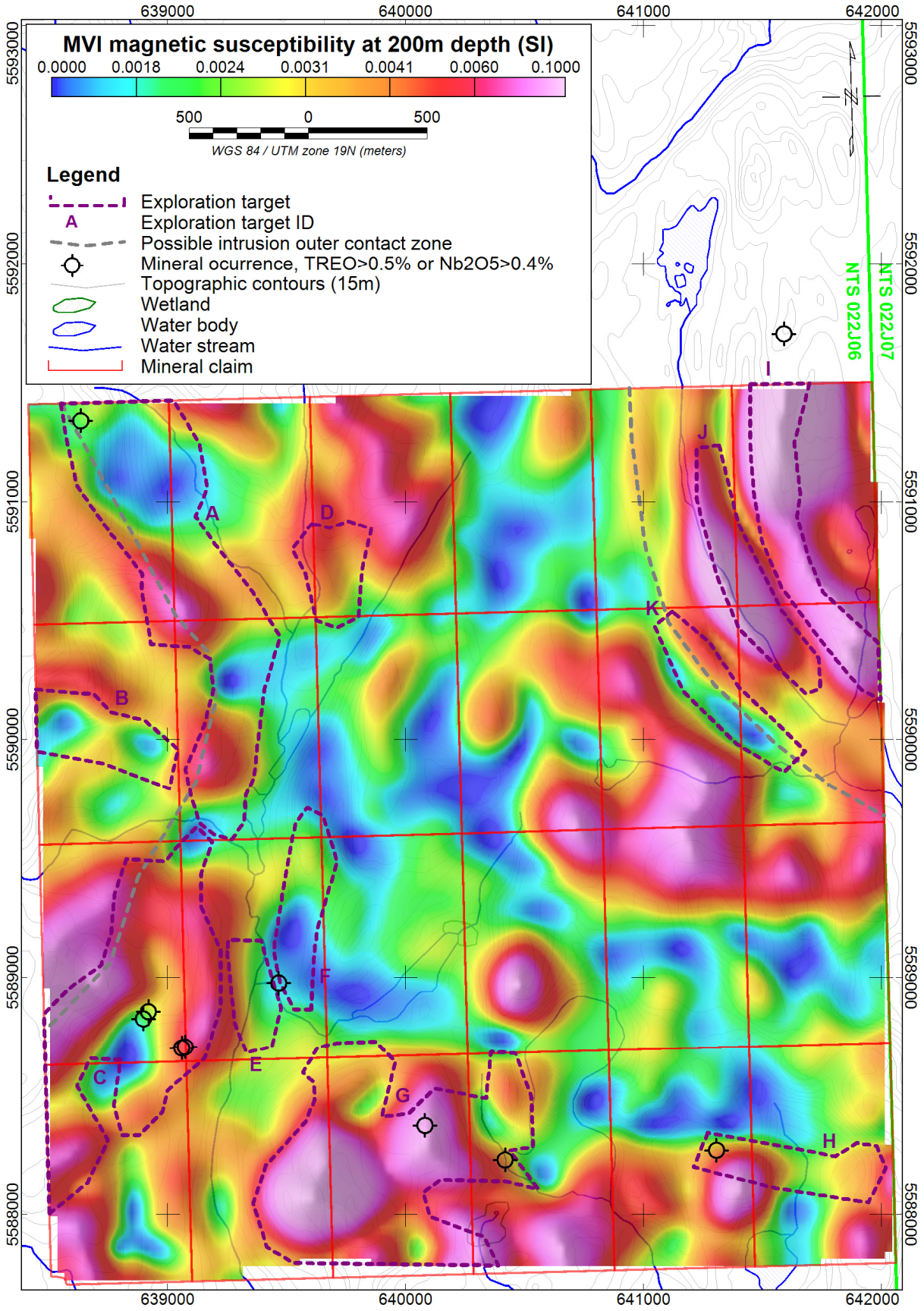

VII. CONCLUSION AND RECOMMENDATIONS

The compilation and magnetic data modeling work has been successful in meeting the mandate objectives. Physical properties were better characterised within the area, which could support a better understanding of the geological setting and the identification of prospective areas. A total of 11 exploration targets have been defined within the Galactic Property for further investigation. A 3D magnetic model of the magnetic susceptibility distribution within the ground is now available for the area and could prove useful for future interpretation and follow-up work.

These targets should be the object of ground prospection campaign, which would require the use of a portable spectrometer device, or at the very least of a handheld scintillometer, in order to ensure that sources of radio-activity can be easily detected and identified on the ground. The implementation of stream sediments, geochemical soil or till sampling programs could also help prioritizing outlined targets, and possibly generate new ones.

Respectfully submitted,

_____

Joël Dubé, P.Eng.
February 10, 2024

VIII. REFERENCES

Ellis, R. G., De Wet, B. and Macleod, I. N., 2012. *Inversion of Magnetic Data from Remanent and Induced Sources*; 22nd International Geophysical Conference and Exhibition, Brisbane.

Lavallée, J-S. et Pacheco, N., 2011. *Rapport de compilation, Propriété J6L1*; Report by Consul-Teck Exploration Inc. for Corporation Éléments Critiques (Québec MERN Sigeom reference GM66291)

Macleod, I. N. and Ellis, R. G., 2013. *Magnetic Vector Inversion, a simple approach to the challenge of varying direction of rock magnetization*; 23rd International Geophysical Conference and Exhibition, Melbourne, ASEG-PESA.

Smith, D., 2011. *Simplified Exploration Work Report, J6L1 Property*; Report by Darren Smith for Claims Hansen (Québec MERN Sigeom reference GM66022)

Stephens, M., 2024. *Helicopter-Borne, Magnetometric and Radiometrics Geophysical Survey, Area Sept-Îles, Québec.* Personal communication.

Vallières, J. et Intissar, R., 2017. *Levé aéromagnétique dans le secteur sud de la rivière Moisie, Côte-Nord*; Report by Québec's MERN (Québec MERN Sigeom reference DP2017-03)

IX. Statement of Qualifications

Joël Dubé
7977 Décarie Drive
Ottawa, ON, Canada, K1C 3K3

Telephone: 819.598.8486
E-mail: jdube@ddgeoscience.ca

I, Joël Dubé, P.Eng., do hereby certify that:

1. I am a consultant in geophysics, President of Dynamic Discovery Geoscience Ltd., registered in Canada.

2. I earned a Bachelor of Engineering in Geological Engineering in 1999 from the École Polytechnique de Montréal.

3. I am an Engineer registered with the Ordre des Ingénieurs du Québec, No. 122937, and a Professional Engineer with Professional Engineers Ontario, No. 100194954 (CofA No. 100219617), with the Association of Professional Engineers and Geoscientists of New Brunswick, No. L5202 (CofA No. F1853), with the Association of Professional Engineers of Nova Scotia, No. 11915 (CofC No. 51099), with Engineers Geoscientists Manitoba, No. 43414. (CofA No. 6897), with Professional Engineers & Geoscientists Newfoundland & Labrador, No. 10012 (PtoP No. N1134) and with the Northwest Territories and Nunavut Association of Professional Engineers & Geoscientists, No. L4447 (PtoP No. P1414)

4. I have practised my profession for 24 years in exploration geophysics.

5. I have not received and do not expect to receive a direct or indirect interest in the properties covered by this report.

Dated this 10th day of February, 2024

_____
Joël Dubé, P.Eng. #122937